11218-3-T = RL-2213

011218-3-T

THE UNIVERSITY OF MICHIGAN

COLLEGE OF ENGINEERING

DEPARTMENT OF ELECTRICAL AND COMPUTER ENGINEERING

Radiation Laboratory

APPLICATION OF THE LARGE GRADIENT VOR ANTENNA

By

Dipak L. Sengupta and Philip Chan

15 March 1973

Interim Engineering Report No. 3

Contract No. DOT-FA72WA-2882
Project No. WA5R-1-0526/N113-739.0

Contract Monitor: Mr. Sterling R. Anderson, RD 331

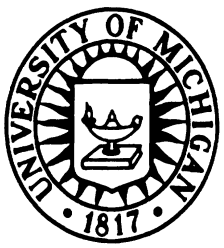

Prepared for:

FEDERAL AVIATION ADMINISTRATION
800 Independence Avenue, S.W.
Washington, D.C. 20591

2216 Space Research Building
2455 Hayward Street
Ann Arbor, Michigan
48105

(313) 764-0500

TABLE OF CONTENTS

LIST OF FIGURE CAPTIONS

1. Coordinate system used.

2. VOR system and scatterer above ground.

3. Direct and reflected rays that reach S.

4. $\alpha_c(\theta)$, $\alpha_s(\theta)$ and $\alpha_s(\theta) - \alpha_c(\theta)$ as functions of θ for a standard VOR antenna in free space. kA = 18.0859, kd = 0.9276, kh = 2.7755, f = 109 MHz.

5. $\alpha_c^T(\theta)$, $\alpha_s^T(\theta)$ and $\alpha_s^T(\theta) - \alpha_c^T(\theta)$ as functions of θ for a standard VOR antenna located 15' above ground. f = 109 MHz.

6. $\alpha_c(\theta)$, $\alpha_s(\theta)$ and $\alpha_s(\theta) - \alpha_c(\theta)$ as functions of θ for a large gradient parasitic antenna in free space. kA = 18.0859, kd = 0.9276, kh = 2.7755, $kH_1 = 3.6$, $kB_1 = 16.9$, $kH_2 = 10.9$, $kB_2 = 12.1$, f = 109 MHz.

7. $\alpha_c^T(\theta)$, $\alpha_s^T(\theta)$ and $\alpha_s^T(\theta) - \alpha_c^T(\theta)$ as functions of θ for a large gradient parasitic loop counterpoise antenna located 15' above ground.

8. Free space scalloping amplitudes $\left|S_1\right|$ and $\left|S_1^{\text{Approx}}\right|$ as functions of $(\phi - \phi_1)$ with A as the parameter.

9. (a) Course scalloping amplitude $\left|S_1\right|$ as a function of $(\phi - \phi_1)$ for a standard VOR antenna located 15' above ground and for different heights of the scatterer. Orbital flight at $\theta = \theta_{\min} \sim 76^\circ$.

9. (b) Course scalloping amplitude $\left|S_2\right|$ as a function of $(\phi - \phi_1)$ for a standard VOR antenna located 15' above ground and for different heights of the scatterer. Orbital flight at $\theta = \theta_{\min} \sim 76^\circ$.

10. (a) Course scalloping amplitude $\left|S_1\right|$ as a function of $(\phi - \phi_1)$ for a standard VOR antenna located 15' above ground and for different heights of the scatterer. Orbital flight at $\theta = \theta_{\max} \sim 83^\circ$.

I

INTRODUCTION

This is the third Interim Report on Contract No. DOT-FA72WA-2882, "Application of the Large Gradient VOR Antenna," and covers the period 1 December 1972 to 28 February 1973.

The present report discusses the theory of course scalloping amplitude in standard VOR bearing indications. Wherever there exists a multipath between a VOR station and a flying aircraft, the multipath signal combines with the desired direct signal to produce various types of siting errors in the VOR indications at the aircraft [1], [2]. Here we discuss only those siting errors which appear as course scalloping in the VOR bearing indications.

Detailed discussions on scalloping amplitude and frequency for a standard VOR system in the presence of various types of multipath signals are given in [2], [4]. The references cited give a considerable amount of observed course scalloping amplitude values produced by different types of scattering objects. Approximate theory of scalloping amplitude has been developed [4] for idealized situations. The theory developed, at its best, is able to explain qualitatively some of the general behavior of the scalloping effects [2], [4]. However, because of the basic approximations made, in many instances [2], [5] the existing theory is unable to explain qualitatively the observed behavior of the course scalloping amplitudes in the various VOR indications.

In the following sections we at first develop a rigorous theory for the course scalloping amplitudes observed in standard VOR indications in the presence of multipath signals. The antenna characteristics, the scattering properties of the multipath sources, and the ground effects are all built into the theory so that their effects on the scalloping may be investigated quantitatively. The analysis assumes that the VOR receiver characteristics are ideal. It is hoped that the theory discussed here may be found useful to analyze the large amount of experimental data on

course scalloping amplitude collected by the FAA over many years [2], [4]. The analytical results discussed below are based on an earlier work by one of the authors [5]. The various approximations involved in the theory are then critically examined. Finally numerical results obtained for a few idealized cases are discussed.

II

FREE SPACE COURSE SCALLOPING AMPLITUDE

2.1 Basic Analysis

In this section theoretical expressions are developed for the course scalloping amplitudes in the standard VOR bearing indications caused by multipath signals when both the VOR station and the scatterer are located in free space. Although this is a very idealized case, the results may be found useful in studying some of the general behavior of the scalloping phenomena.

Let us assume that the VOR station is located at the origin O of a rectangular coordinate system x, y, z (Fig. 1). A stationary aircraft is located at the far field

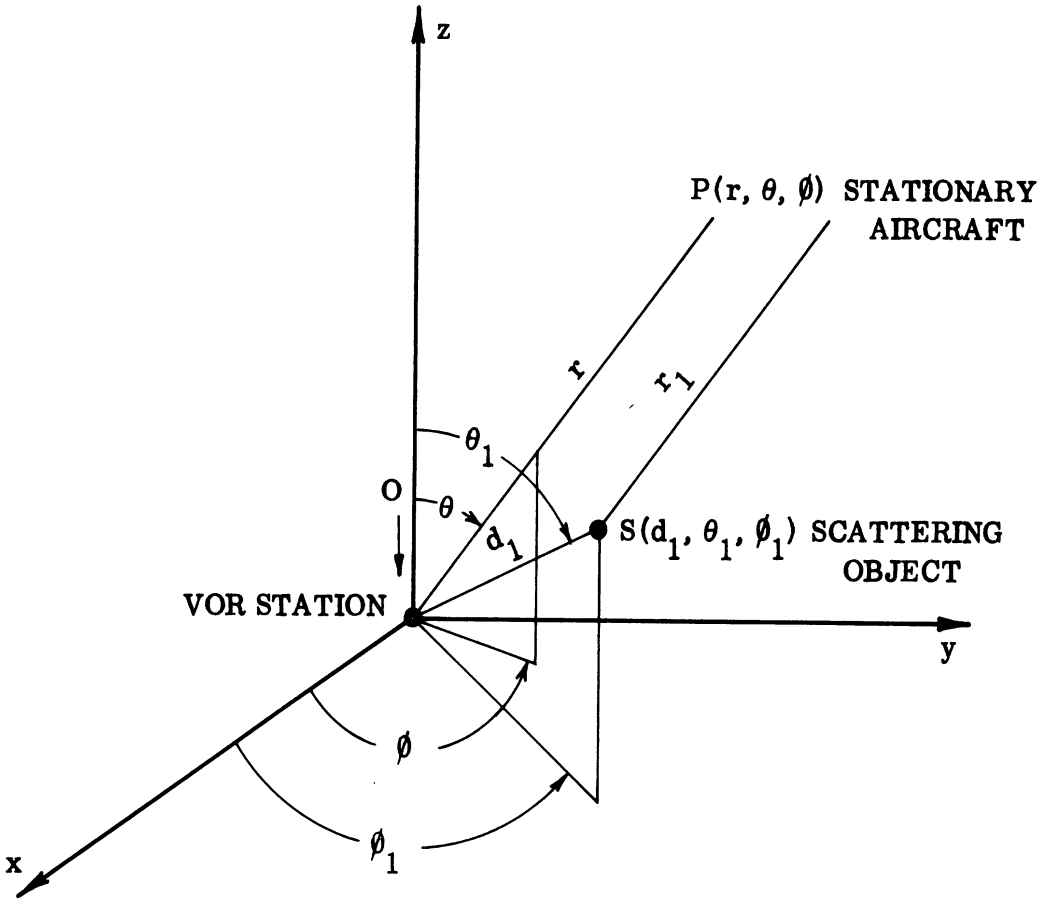

Fig. 1: Coordinate system used.

point P whose coordinates are (r, θ, ϕ) expressed in spherical polar coordinates with origin at O. A scattering object is located at S which is represented by the coordinates (d_1, θ_1, ϕ_1). It is assumed that the distance of the scatterer from the VOR station is sufficiently large $(kd_1 \gg 1)$ so that the usual geometrical optics approximation may be used in obtaining the field incident at S. We assume here that the field radiated by the VOR antenna system is horizontally polarized and that the scattering object does not produce any depolarization of the field.

The direct signal at P coming from the VOR station may be written as:

$$E_d(P) = K \frac{e^{-i(\omega t - kr)}}{r} \left[S_c(\theta) + S_s(\theta) \cos(\omega_m t - \phi) \right] , \qquad (1)$$

where,

K is a constant,

ω is the carrier frequency in radians,

$k = 2\pi/\lambda$ is the propagation constant in free space,

ω_m is the modulating frequency in radians,

$S_c(\theta)$ is the free space elevation plane complex far field pattern of the VOR antenna in the carrier mode,

$S_s(\theta)$ is the free space elevation plane complex far field pattern of the VOR antenna in the side-band mode.

Notice that in Eq. (1) the modulation index 'm' of the space amplitude modulated wave is not explicitly stated. However, this can be assumed to be included as an appropriate multiplying factor in $S_s(\theta)$. Observe that, as indicated by Eq. (1), the side-band and carrier signals are not in general r.f. phase with each other. The implications of the r.f. phase relationship between the carrier and side-band signals will be discussed later in more detail. Explicit expressions for the standard VOR antenna complex pattern functions have been discussed elsewhere [6], [7]. It will be assumed that $S_c(\theta)$ and $S_s(\theta)$ are known in the present problem.

For later reference we write the pattern functions in the following way:

$$S_c(\theta) = \left| S_c(\theta) \right| e^{i\alpha_c(\theta)} \tag{2}$$

$$S_s(\theta) = \left| S_s(\theta) \right| e^{i\alpha_s(\theta)} \quad . \tag{3}$$

In the absence of any other signal, the VOR receiver at P detects the envelope of Eq. (1) and observes the phase ϕ of the detected signal which gives the azimuth of the field point P with respect to the VOR station. However, in the presence of multipath signals, the phase relationship between the carrier and side-band signals are disturbed thereby producing errors in the azimuth information indicated by the receiver.

The field incident at the scattering object S, located sufficiently far from the VOR station, may be written as follows:

$$E_i(S) = K \cdot \frac{e^{-i(\omega t - kd_1)}}{d_1} \left[S_c(\theta_1) + S_s(\theta_1) \cos(\omega_m t - \phi_1) \right] \quad , \tag{4}$$

where the various notations are as explained before. The multipath signals at P will be that portion of field, given by Eq. (4), scattered by the scattering object S in the direction of P. For a finite object the scattered field at P will appear as a spherical wave originating from S. It can be shown that the multipath signal at P may be expressed [5] as follows:

$$E_s(P) = K \cdot \frac{e^{-i\left[\omega t - k(r_1 + d_1)\right]}}{r_1} A(\theta_1, \phi_1, d_1; \theta, \phi - \phi_1) e^{i\delta} \, x$$

$$x \left[S_c(\theta_1) + S_s(\theta_1) \cos(\omega_m t - \phi_1) \right] \quad , \tag{5}$$

where,

r_1 is the distance between the scattering object and the aircraft at P, $A(\theta_1, \phi_1, d_1; \theta, \phi-\phi_1)\, e^{i\delta}$ may be identified with the scattering or reflecting properties of the scatterer. The dependence of the incident and scattering angles as well as the distance d_1 of the scatterer from the VOR antenna are explicitly written in A to emphasize the fact that in many cases of practical interest the scattered field from the object depends strongly on these parameters For convenience we shall, from now on, suppress the variables $\theta_1, \phi_1, d_1, \theta, \phi$ from A.

In Eq. (5) A and δ may be identified respectively with the amplitude and phase of the scattering coefficient of the object. By definition both A and δ are real quantities.

Since P is located in the far zones of both the VOR antenna and the multipath object S, we can make the usual far field approximations and can rewrite Eq. (5) in the following form:

$$E_s(P) = K\frac{e^{-i(\omega t - kr)}}{r} A\, e^{i\xi} \; x$$

$$x \left[S_c(\theta_1) + S_s(\theta_1) \cos(\omega_m t - \phi_1) \right] , \tag{6}$$

where,

$$\xi = kd_1(1 - \cos\gamma) + \delta \tag{7}$$

$$\cos\gamma = \sin\theta \sin\theta_1 \cos(\phi - \phi_1) + \cos\theta \cos\theta_1 . \tag{8}$$

The total field received at P is obtained by adding Eqs. (1) and (6) and is given by:

$$E(P) = K\frac{e^{-i(\omega t - kr)}}{r} S_c(\theta) \left[1 + A\, e^{i\xi} \frac{S_c(\theta_1)}{S_c(\theta)} + \right.$$

$$\left. + \frac{S_s(\theta)}{S_c(\theta)} \cos(\omega_m t - \phi) + A\, e^{i\xi} \frac{S_c(\theta_1)}{S_c(\theta)} \cos(\omega_m t - \phi_1) \right] . \tag{9}$$

After some algebraic manipulations, Eq. (9) may be written in the following form:

$$E(P) = K \cdot \frac{e^{-i\left[\omega t - kr - \alpha_c(\theta) - \xi\right]}}{r} \left|S_c(\theta)\right| \times \left[f_c + f_s\right], \tag{10}$$

where,

$$f_c^2 = 1 + A^2 \left|\frac{S_c(\theta_1)}{S_c(\theta)}\right|^2 + 2A \left|\frac{S_c(\theta_1)}{S_c(\theta)}\right| \cos\left[\xi + \alpha_c(\theta_1) - \alpha_c(\theta)\right], \tag{11}$$

$$\tan\zeta = \frac{A\left|\frac{S_c(\theta_1)}{S_c(\theta)}\right| \sin\left[\xi + \alpha_c(\theta_1) - \alpha_c(\theta)\right]}{1 + A\left|\frac{S_c(\theta_1)}{S_c(\theta)}\right| \cos\left[\xi + \alpha_c(\theta_1) - \alpha_c(\theta)\right]} \tag{12}$$

$$f_s = \frac{S_s(\theta)}{S_c(\theta)} e^{-i\zeta} \cos(\omega_m t - \phi) + A \frac{S_s(\theta_1)}{S_c(\theta)} e^{i(\xi - \zeta)} \cos(\omega_m t - \phi_1) . \tag{13}$$

In Eq. (10) f_c may be identified with the combined carrier signals at P and it contains no azimuth information. Similarly f_s may be identified with the combined side-band signals at P which contain the azimuth information of the VOR and the scattering object. The detector output at the ideal VOR receiver at P is proportional to the real part of f_s. Let us denote f = Real part of f_s given by Eq. (13). It can be shown that f can be written as:

$$f = N \cos(\omega_m t - \phi + \alpha) , \tag{14}$$

where,

$$N^2 = \left|\frac{S_s(\theta)}{S_c(\theta)}\right|^2 \cos^2\left[\alpha_s(\theta) - \alpha_c(\theta) - \zeta\right]$$

$$+ A^2 \left|\frac{S_s(\theta_1)}{S_c(\theta)}\right|^2 \cos^2\left[\alpha_s(\theta_1) - \alpha_c(\theta) + \xi - \zeta\right] +$$

$$+ 2A \left|\frac{S_s(\theta)}{S_c(\theta)}\right| \left|\frac{S_s(\theta_1)}{S_c(\theta)}\right| \cos\left[\alpha_s(\theta) - \alpha_c(\theta) - \zeta\right]$$

$$\times \cos\left[\alpha_s(\theta_1) - \alpha_c(\theta_1) + \xi - \zeta\right] \cos(\phi - \phi_1), \qquad (15)$$

$$\tan\alpha = \frac{A\left|\frac{S_s(\theta_1)}{S_c(\theta)}\right| \cos\left[\alpha_s(\theta_1) - \alpha_c(\theta) + \xi - \zeta\right] \sin(\phi - \phi_1)}{\left|\frac{S_s(\theta)}{S_c(\theta)}\right| \cos\left[\alpha_s(\theta) - \alpha_c(\theta) - \zeta\right] + A\left|\frac{S_s(\theta_1)}{S_c(\theta)}\right| \cos\left[\alpha_s(\theta_1) - \alpha_c(\theta) + \xi - \zeta\right] \cos(\phi - \phi_1)} . \qquad (16)$$

The bearing indication in the VOR receiver is given by the phase of Eq. (14). Thus we can write the bearing indication B as given by:

$$B = \phi - \alpha \quad . \qquad (17)$$

The true bearing of the aircraft with respect to the VOR station is ϕ. Note that in the absence of multipath signals, $A = 0$ and Eq. (14) takes the following form:

$$f = \left|\frac{S_s(\theta)}{S_c(\theta)}\right| \cos\left[\alpha_s(\theta) - \alpha_c(\theta)\right] \cos(\omega_m t - \phi) \quad . \qquad (18)$$

Equation (18) indicates that the detected signal amplitude depends quite strongly on the r.f. phase relationship between the carrier and side-band signals. From the point of view of detection maximum efficiency will occur if $\alpha_c(\theta) = \alpha_s(\theta)$, i.e., the carrier and side-band signals are in phase at all angles θ. In general, $\alpha_s(\theta) \neq \alpha_c(\theta)$. It is possible to adjust the phase relationship such that $\alpha_s(\theta_o) - \alpha_c(\theta_o) = 0$ in a certain direction $\theta = \theta_o$. However, since $\alpha_s(\theta) - \alpha_c(\theta)$ changes with θ, the phase adjustments made at $\theta = \theta_o$, will be disturbed at angles $\theta \neq \theta_o$. As we shall see later, this aspect of the phase relationship will have considerable effects on the scalloping amplitudes in the presence of multipath signals.

Thus the second term in Eq. (17) may be considered as the bearing error. Let us write the bearing indication of the VOR receiver at the aircraft as:

$$B = \phi + \Delta\phi \quad , \tag{19}$$

where $\Delta\phi$ is the error introduced due to the multipath signal. Complete expression for the error $\Delta\phi$ is given by:

$$\Delta\phi = -\alpha = -\tan^{-1} \frac{A\left|\frac{S_c(\theta_1)}{S_c(\theta)}\right|\left[\cos\ \alpha_s(\theta_1) - \alpha_c(\theta) + \xi - \zeta\right] \sin(\phi - \phi_1)}{\left|\frac{S_s(\theta)}{S_c(\theta)}\right| \cos\left[\alpha_s(\theta) - \alpha_c(\theta) - \zeta\right] + A\left|\frac{S_d(\theta_1)}{S_c(\theta)}\right| \cos\left[\alpha_s(\theta_1) - \alpha_c(\theta) + \xi - \zeta\right] \cos(\phi - \phi_1)} \quad . \tag{20}$$

Note that in the absence of multipath signal $A = 0$ and hence from Eq. (20) it follows that $\Delta\phi = 0$. For convenience of reference and later discussion, we rewrite below the explicit expressions for ξ and ζ given earlier:

$$\xi = kd_1\left[1 - \sin\theta \sin\theta_1 \cos(\phi - \phi_1) - \cos\theta \cos\theta_1\right] + \delta \quad , \tag{21}$$

$$\zeta = \tan^{-1} \frac{A\left|\frac{S_c(\theta_1)}{S_c(\theta)}\right| \sin\left[\xi + \alpha_c(\theta_1) - \alpha_c(\theta)\right]}{1 + A\left|\frac{S_c(\theta_1)}{S_c(\theta)}\right| \cos\left[\xi + \alpha_c(\theta_1) - \alpha_c(\theta)\right]} \quad . \tag{22}$$

2.2 Free Space Course Scalloping Amplitude

In the presence of multipath signal the bearing error in the VOR indications of a stationary aircraft located at (r, θ, ϕ) with respect to the VOR station is given by Eq. (20) As the aircraft flies $\Delta\phi$ will change due to the variation of the parameters θ and ϕ. For a radial flight with respect to the VOR station θ is variable

and ϕ is constant. Whereas for an orbital flight at constant height θ is constant but ϕ is variable. In both cases $\Delta\phi$ changes above and below the true value of ϕ with variation of the coordinates θ and ϕ of the flying aircraft.

Before investigating the nature of variation of $\Delta\phi$ it is instructive to study the variations of the parameters ξ and ζ (in Eq. (20)) with the aircraft motion. If $A\left|\frac{S_c(\theta_1)}{S_c(\theta)}\right| \ll 1$, which is a reasonable approximation, Eq. (22) indicates that ζ is a small quantity ($\zeta \ll 1$) and the effects of its variation with the aircraft motion on the final results may be assumed negligible. The parameter ξ, given by Eq. (21), is large and its variation with ϕ is also large. As a result, the terms involving ξ in Eq. (20) oscillates between +1 and -1 as the aircraft moves. Thus the variation of $\Delta\phi$ with the aircraft motion will be a slow variation with ϕ (or θ as the case may be), determined by the terms $\sin(\phi-\phi_1)$ and $\cos(\phi-\phi_1)$ in Eq. (20) mounted on top an oscillatory variation determined mainly by the parameter ξ. It is evident that $\Delta\phi$ fluctuates between positive and negative values with the motion of the aircraft. The amplitudes of these positive and negative swings of the error $\Delta\phi$ are termed as course scalloping amplitudes. We write the bearing indications of the VOR receiver at the flying aircraft as:

$$B = \phi - S_{1,2} \quad , \tag{23}$$

where,

S_1 is the value of $\Delta\phi$ obtained from Eq. (20) when $\cos\left[\alpha_s(\theta_1) - \alpha_c(\theta) + \xi - \zeta\right] = 1$,

S_2 is the value of $\Delta\phi$ obtained from Eq. (23) when $\cos\left[\alpha_s(\theta_1) - \alpha_c(\theta) + \xi - \zeta\right] = -1$.

S_1, S_2 may be called the course scalloping amplitudes which give the two bounds of the scalloping errors as the aircraft moves. Note that S_1 and S_2 are of opposite signs and in general $|S_1| \neq |S_2|$.

By definition,

$$S_1 = \Delta\phi \text{ evaluated at } \xi = \xi_{01},\ \zeta = \zeta_{01}, \tag{24}$$

where,

$$\alpha_s(\theta_1) - \alpha_c(\theta) + \xi_{01} - \zeta_{01} = 2n\pi \quad , \quad n \text{ is a positive integer} \tag{25}$$

$$\tan \zeta_{01} = \frac{A\left|\frac{S_c(\theta_1)}{S_c(\theta)}\right| \sin\left[\xi_{01} + \alpha_c(\theta_1) - \alpha_c(\theta)\right]}{1 + A\left|\frac{S_c(\theta_1)}{S_c(\theta)}\right| \cos\left[\xi_{01} + \alpha_c(\theta_1) - \alpha_c(\theta)\right]} \quad . \tag{26}$$

Equation (26) can be solved for ζ_{01} and we obtain:

$$\zeta_{01} = -\sin^{-1}\left[A\left|\frac{S_c(\theta_1)}{S_c(\theta)}\right| \sin^{-1}\left\{\alpha_s(\theta_1) - \alpha_c(\theta_1)\right\}\right] \quad . \tag{27}$$

After using Eqs. (20), (24)-(27) the following is obtained:

$$S_1 = -\tan^{-1}\frac{A\left|\frac{S_s(\theta_1)}{S_c(\theta)}\right| \sin(\phi - \phi_1)}{\left|\frac{S_s(\theta)}{S_c(\theta)}\right| \cos\left[\alpha_s(\theta) - \alpha_c(\theta) - \zeta_{01}\right] + A\left|\frac{S_s(\theta_1)}{S_c(\theta)}\right| \cos(\phi - \phi_1)} \quad . \tag{28}$$

Similarly, S_2 is obtained from Eq. (20) for values $\xi = \xi_{02}$, $\zeta = \zeta_{02}$ given by

$$\alpha_s(\theta_1) - \alpha_c(\theta) + \xi_{02} - \zeta_{02} = n\pi \quad , \quad n \text{ is a positive odd number} \tag{29}$$

$$\tan \zeta_{02} = \frac{A\left|\frac{S_c(\theta_1)}{S_c(\theta)}\right| \sin\left[\xi_{02} + \alpha_c(\theta_1) - \alpha_c(\theta)\right]}{1 + A\left|\frac{S_c(\theta_1)}{S_c(\theta)}\right| \cos\left[\xi_{02} + \alpha_c(\theta_1) - \alpha_c(\theta)\right]} \quad . \tag{30}$$

Equation (30) has the solution:

$$\zeta_{02} = \sin^{-1}\left[A\left|\frac{S_c(\theta_1)}{S_c(\theta)}\right|\sin\left\{\alpha_s(\theta_1)-\alpha_c(\theta_1)\right\}\right] \quad . \tag{31}$$

Proceeding as before we obtain:

$$S_2 = \tan^{-1}\frac{A\left|\frac{S_s(\theta_1)}{S_c(\theta)}\right|\sin(\phi-\phi_1)}{\left|\frac{S_s(\theta)}{S_c(\theta)}\right|\cos\left[\alpha_s(\theta)-\alpha_c(\theta)-\zeta_{02}\right]-A\left|\frac{S_s(\theta_1)}{S_c(\theta)}\right|\cos(\phi-\phi_1)} \quad . \tag{32}$$

2.3 Discussion of Free Space Course Scalloping Amplitude

Approximate course scalloping amplitude expressions are given in VOR Handbook [2]. In this section we discuss in the light of the theory discussed in the previous sections, the scalloping amplitude expression given in [2] for the case of a non-directional multipath source. In particular we discuss Eq. (4-1) on page 22 of [2]. The physical arrangement of the VOR station, the multipath source and the aircraft considered in [2] implies in our present notation:

$$\theta = \theta_1 = \pi/2 \quad ,$$

$$A \text{ is a constant,}$$

$$\delta = 0 \quad .$$

Thus we obtain the following from Eqs. (28) and (29):

$$S_1 = -\tan^{-1}\frac{A\sin(\phi-\phi_1)}{\left[\cos\ \alpha_s(\pi/2)-\alpha_c(\pi/2)+\sin^{-1}\left\{A\sin(\alpha_s(\pi/2)-\alpha_c(\pi/2))\right\}\right]+A\cos(\phi-\phi_1)} \tag{33}$$

$$S_2 = \tan^{-1}\frac{A\sin(\phi-\phi_1)}{\left[\cos\ \alpha_s(\pi/2)-\alpha_c(\pi/2)-\sin^{-1}\left\{A\sin(\alpha_s(\pi/2)-\alpha_c(\pi/2))\right\}\right]-A\cos(\phi-\phi_1)} \tag{34}$$

If it is now assumed that $\alpha_s(\pi/2) = \alpha_c(\pi/2)$ which implies that the side-band and carrier mode fields are in phase in the direction of $\theta = \pi/2$, Eq. (33) and (34) reduce to the following:

$$S_1 = -\tan^{-1}\frac{A\sin(\phi-\phi_1)}{1+A\cos(\phi-\phi_1)} \tag{35}$$

$$S_2 = \tan^{-1}\frac{A\sin(\phi-\phi_1)}{1-A\cos(\phi-\phi_1)} \tag{36}$$

Under the assumption of $A \ll 1$, Eqs. (35) and (36) reduce to Eq. (4-1) given in [2] which is:

$$\begin{aligned} S_1 &\simeq +\tan^{-1} A\sin(\phi-\phi_1) \\ {}^{2} &\simeq +A\sin(\phi-\phi_1), \text{ for } A \ll 1. \end{aligned} \tag{37}$$

If $\alpha_s \neq \alpha_c$, which is most certainly possible in a real case, Eq. (37) will give values which are too low for scalloping amplitudes even under the assumption of $A \ll 1$. To show this we assume

$$\begin{aligned} &\left|\alpha_s(\pi/2) - \alpha_c(\pi/2)\right| \gg 0 \ , \\ &A \ll 1 \ . \end{aligned} \tag{38}$$

Under the conditions (38) it can be shown that S_1, S_2 as given by Eqs. (33) and (34) are given by:

$$\begin{matrix} S_1 \\ 2 \end{matrix} = \mp\tan^{-1}\frac{A\sin(\phi-\phi_1)}{\cos\left[\alpha_s(\pi/2) - \alpha_c(\pi/2)\right] \pm A\cos(\phi-\phi_1)} \ . \tag{39}$$

Hence unless $\alpha_s(\pi/2) - \alpha_c(\pi/2) = \pm n\pi$, the neglect of $A\cos(\phi-\phi_1)$ and the assumption of $\cos\left[\alpha_s(\pi/2) - \alpha_c(\pi/2)\right] = 1$ in the denominator of Eq. (39) are not justified. Thus in general the values predicted by Eqs. (35)-(37) will be lower than those predicted

by Eq. (39).

On the basis of the free space theory developed and the discussion given here, it appears that the side-band and carrier mode elevation plane complex patterns (in particular, their phases) should be considered in evaluating the course scalloping amplitudes.

III

COURSE SCALLOPING AMPLITUDE IN THE PRESENCE OF A GROUND

In this section we generalize the theory of VOR course scalloping amplitude to the case when the VOR station and the source of multipath signal are located above a perfectly conducting infinite planar ground. This is a more realistic case and is of considerable practical interest. Figure 2 represents geometrically the arrangement of the problem to be studied. The VOR antenna is located at $(Z_o, 0, 0)$, the scatterer at (d_1, θ_1, ϕ_1) and the ground plane is at $z = 0$. The free space theory is generalized to the present case by taking into account the image fields produced at P by the perfectly conducting ground.

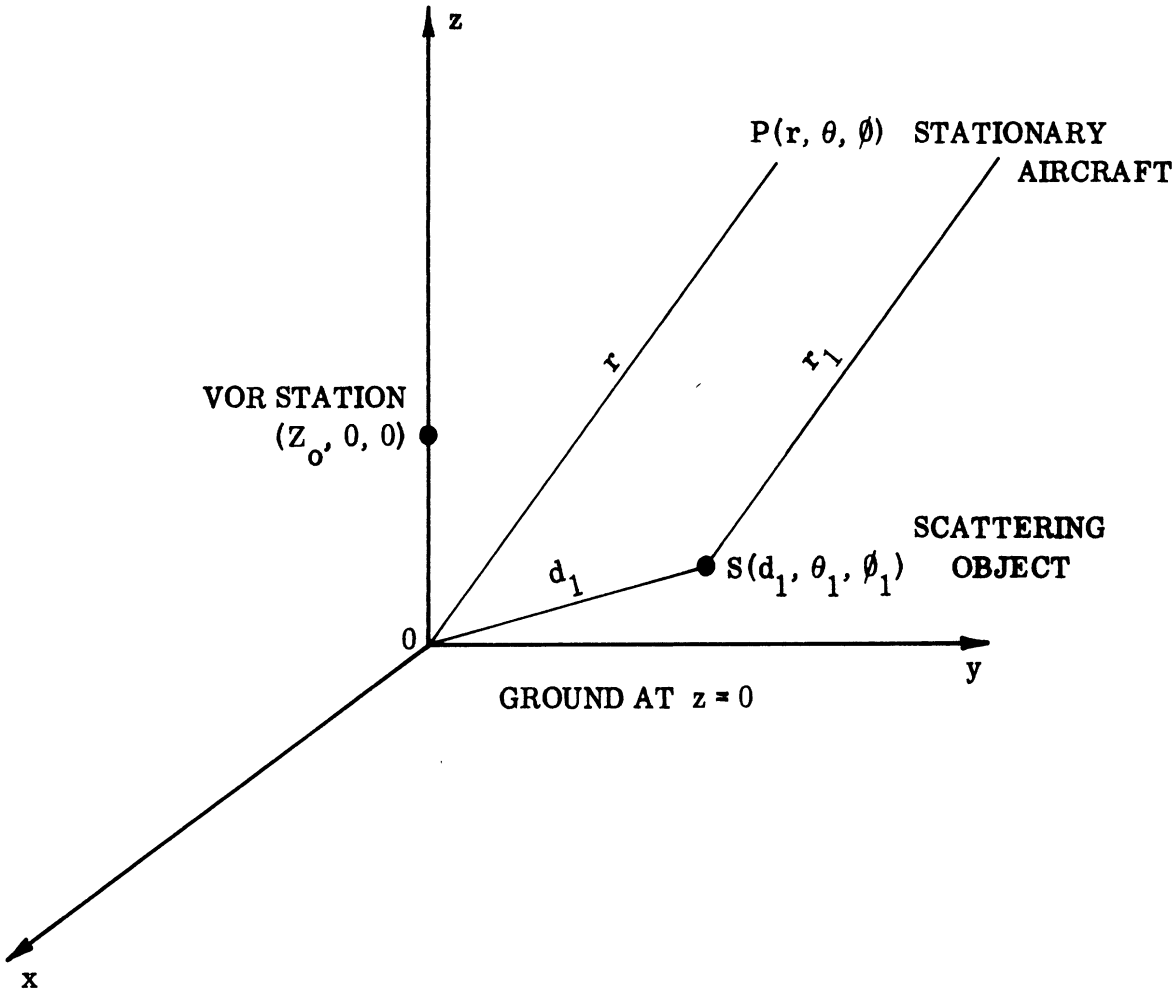

Fig. 2: VOR system and scatterer above ground.

The field at P due to the VOR station alone may be written as:

$$E_d(P) = K \cdot \frac{e^{-i(\omega t - kr)}}{r} \left[S_c^T(\theta) + S_s^T(\theta) \cos(\omega_m t - \phi) \right] , \quad (40)$$

where,

$$S_c^T(\theta) = S_c(\theta)\, e^{-ikZ_o \cos\theta} - S_c(\pi - \theta)\, e^{ikZ_o \cos\theta} , \quad (41)$$

$$S_s^T(\theta) = S_s(\theta)\, e^{ikZ_o \cos\theta} - S_s(\pi - \theta)\, e^{ikZ_o \cos\theta} , \quad (42)$$

where $S_c(\theta)$, $S_s(\theta)$ are the free space elevation plane complex far field patterns of the VOR antenna in carrier and side-band modes respectively.

The derivation of the multipath signal at P is more complicated and is discussed in more detail in the following section.

3.1 Multipath Signal at P

At first we need the field incident at S from the VOR antenna. If S is in the far zone of the antenna then it can be obtained from Eq. (40). We assume here that S is not in the far zone but it is sufficiently far away from the VOR station so that $kd_1 \gg 1$. Under this condition usual geometrical optics approximations can be used To obtain the incident field $E_i(S)$ we consider the direct and reflected waves originating from the VOR and reaching the scatterer S (Fig. 3). The incident field at S can be written as:

$$E_i(S) = K \cdot \frac{e^{-i(\omega t - kd_1')}}{d_1'} f(\theta_1', \phi_1) - K \frac{e^{-i(\omega t - kd_1'')}}{d_1''} f(\pi - \theta_1'', \phi) , \quad (43)$$

where,

$$f(\theta, \phi) = S_c(\theta) + S_s(\theta) \cos(\omega_m t - \phi) . \quad (44)$$

From Fig. 3 it can be shown that

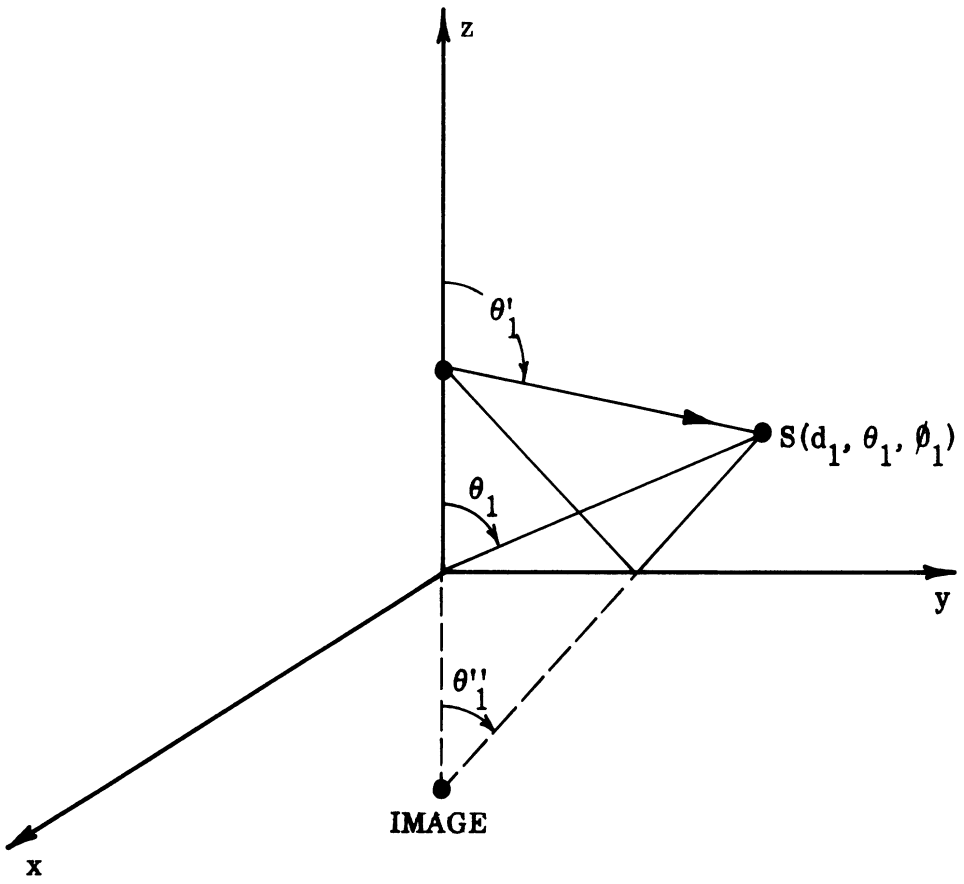

Fig. 3: Direct and reflected rays that reach S.

$$\left.\begin{aligned} d'_1 &\simeq d_1\left(1-\frac{Z_o}{d_1}\cos\theta_1\right) \\ d''_1 &\simeq d_1\left(1+\frac{Z_o}{d_1}\cos\theta_1\right) \end{aligned}\right\} \quad \text{for } \frac{Z_o}{d_1} \ll 1 \tag{45}$$

and,

$$\left.\begin{aligned} \sin\theta'_1 &\simeq \frac{\sin\theta_1}{1+\frac{Z_o}{d_1}\cos\theta_1} \\ \sin\theta''_1 &\simeq \frac{\sin\theta_1}{1+\frac{Z_o}{d_1}\cos\theta_1} \end{aligned}\right\} \quad \text{for } \frac{Z_o}{d_1} \ll 1 \ . \tag{46}$$

If the scatterer S is located at a distance D from the z-axis and at a height H above the ground plane then it can be shown that:

$$\left.\begin{aligned} \tan\theta_1 &= \frac{D}{H} \\ d_1\cos\theta_1 &= H \\ d_1\cos\theta_1 &= D \end{aligned}\right\} \quad . \tag{47}$$

After using Eqs. (45) and (46), Eq. (43) can be written as follows:

$$E_i(S) = K\cdot e^{-i\omega t}\,\frac{e^{ikd_1\left(1-\frac{Z_o}{d_1}\cos\theta_1\right)}}{d_1\left(1-\frac{Z_o}{d_1}\cos\theta_1\right)}\, f(\theta_1', \phi_1) -$$

$$- K\cdot e^{-i\omega t}\,\frac{e^{ikd_1\left(1+\frac{Z_o}{d_1}\cos\theta_1\right)}}{d_1\left(1+\frac{Z_o}{d_1}\cos\theta_1\right)}\, f(\pi-\theta_1'', \phi_1) \quad . \tag{48}$$

As before we assume that the scattered field at P is related to $E_i(S)$ by:

$$E_s'(P) = E_i(S)\, A(\theta_1, \phi_1; \theta, \phi)\, e^{i\delta}\,\frac{e^{ikr_1}}{r_1} \quad . \tag{49}$$

In obtaining the scattered field at P we must take into account the effect of the ground. In this case we can assume that P is located in the far zone of S and the usual far zone approximations may be made. The total scattered or multipath signal at P is then obtained as in the following:

$$E_s(P) = K \cdot \frac{e^{-i(\omega t - kr)}}{r} A \left[\frac{e^{-ikZ_o \cos\theta_1}}{1 - \frac{Z_o}{d_1}\cos\theta_1} f(\theta_1', \phi_1) - \frac{e^{ikZ_o \cos\theta_1}}{1 + \frac{Z_o}{d_1}\cos\theta_1} f(\pi - \theta_1'', \phi_1) \right] \left[e^{i\{kd_1(1-\cos\gamma)+\delta\}} - e^{i\{kd_1(1-\cos\gamma')+\delta\}} \right], \quad (50)$$

where,

$$\left.\begin{aligned} \cos\gamma &= \sin\theta \sin\theta_1 \cos(\phi - \phi_1) + \cos\theta\cos\theta_1 \\ \cos\gamma' &= \sin\theta \sin\theta_1 \cos(\phi - \phi_1) - \cos\theta\cos\theta_1 \end{aligned}\right\} . \quad (51)$$

After some algebraic manipulations Eq. (50) can be rearranged in the following form:

$$E_s(P) = K \cdot \frac{e^{-i(\omega t - kr)}}{r} 2A \sin(kH\cos\theta)\, e^{i\xi'} \sin(kH\cos\theta) \quad x$$

$$x \left[\frac{e^{ikZ_o\cos\theta_1}}{1 - \frac{Z_o}{d_1}\cos\theta_1} f(\theta_1', \phi_1) - \frac{e^{ikZ_o\cos\theta_1}}{1 + \frac{Z_o}{d_1}\cos\theta_1} f(\pi - \theta_1'', \phi_1) \right] , \quad (52)$$

where,

$$\xi' = kd_1 \left[1 - \sin\theta \sin\theta_1 \cos(\phi - \phi_1) \right] + \delta - \pi/2 . \quad (53)$$

In many practical situations $\frac{Z_o}{d_1} \ll 1$ and we can neglect the terms $\frac{Z_o}{d_1}\cos\theta_1$ in the denominators of the terms within parenthesis in Eq. (12) and also can write $\theta_1' \simeq \theta_1'' \simeq \theta_1$. Under these conditions Eq. (52) simplifies to the following:

$$E_s(P) = K \cdot \frac{e^{-i(\omega t - kr)}}{r} 2A\, e^{i\xi'} \sin(kH\cos\theta) \quad x$$

$$x \left[S_c^T(\theta_1) + S_s^T(\theta_1) \cos(\omega_m t - \phi_1) \right] , \tag{54}$$

where $S_c^T(\theta)$ and $S_s^T(\theta)$ are as defined by Eqs. (41) and (42).

We shall use the simplified expression given by Eq. (54) for the scattered field at P instead of the more accurate expression given by Eq. (52) which is given here in case it is needed for more accurate results.

3.2 Total Field at the Far Field Point and the Bearing Error

The total field at P is obtained by combining Eqs (40) and (54) and is given by:

$$E(P) = K \cdot \frac{e^{-i(\omega t - kr)}}{r} S_c^T(\theta) \quad x$$

$$x \left[1 + 2A\, e^{i\xi'} \cdot \frac{S_c^T(\theta_1)}{S_c^T(\theta)} \sin(kH\cos\theta) \right.$$

$$+ \frac{S_s^T(\theta)}{S_s^T(\theta)} \cos(\theta_m t - \phi)$$

$$\left. + 2A\, e^{i\xi'} \frac{S_s^T(\theta_1)}{S_c^T(\theta)} \sin(kH\cos\theta) \cos(\omega_m t - \phi_1) \right] . \tag{55}$$

After some algebraic manipulations Eq. (55) may be rearranged as follows:

$$E(P) = K \cdot \frac{e^{-i(\omega t - kr - \alpha_c^T(\theta) - \zeta'}}{r} \left| S_c^T(\theta) \right| \quad x \left[f_c' + f_s' \right] , \tag{56}$$

where,

$$(f_c')^2 = 1+4A^2\left|\frac{S_c^T(\theta_1)}{S_c^T(\theta)}\right|^2 \sin^2(kH\cos\theta) +$$

$$+4A\left|\frac{S_c^T(\theta_1)}{S_c^T(\theta)}\right| \sin(kH\cos\theta)\cos\left\{\xi'+\alpha_c^T(\theta_1)-\alpha_c^T(\theta)\right\}, \qquad (57)$$

$$\tan\zeta' = \frac{2A\left|\frac{S_c^T(\theta_1)}{S_c^T(\theta)}\right| \sin(kH\cos\theta)\sin\left\{\xi'+\alpha_c^T(\theta_1)-\alpha_c^T(\theta)\right\}}{1+2A\left|\frac{S_c^T(\theta_1)}{S_c^T(\theta)}\right| \sin(kH\cos\theta)\cos\left\{\xi'+\alpha_c^T(\theta_1)-\alpha_c^T(\theta)\right\}}, \qquad (58)$$

$$f_s' = \frac{S_s^T(\theta)}{S_c^T(\theta)} e^{-i\zeta'}\cos(\omega_m t-\phi) +$$

$$+2A\left|\frac{S_s^T(\theta_1)}{S_c^T(\theta)}\right| \sin(kH\cos\theta)\, e^{i(\xi'-\zeta')}\cos(\omega_m t-\phi_1), \qquad (59)$$

$$\left.\begin{aligned} S_c^T(\theta) &= \left|S_c^T(\theta)\right| e^{i\alpha_c^T(\theta)} \\ S_s^T(\theta) &= \left|S_s^T(\theta)\right| e^{i\alpha_s^T(\theta)} \end{aligned}\right\}. \qquad (60)$$

As before, let f' = Real part of f_s'. From Eq. (59) we obtain the following expression for f':

$$f' = \left|\frac{S_s^T(\theta)}{S_c^T(\theta)}\right| \cos\left[\alpha_s^T(\theta) - \alpha_c^T(\theta) - \zeta'\right] \cos(\omega_m t - \phi) +$$

$$+ 2A\left|\frac{S_s^T(\theta_1)}{S_c^T(\theta)}\right| \sin(kH\cos\theta) \cos\left[\alpha_s^T(\theta_1) - \alpha_c^T(\theta) + \xi' - \zeta'\right] \cos(\omega_m t - \phi_1) \quad . \tag{61}$$

We now express f' in the following term:

$$f' = N' \cos(\omega_m t - \phi + \alpha') \quad , \tag{62}$$

where,

$$(N')^2 = \left|\frac{S_s^T(\theta)}{S_c^T(\theta)}\right|^2 \cos^2\left[\alpha_s^T(\theta) - \alpha_c^T(\theta) - \zeta'\right] +$$

$$+ 4A^2 \sin^2(kH\cos\theta) \left|\frac{S_s^T(\theta_1)}{S_c^T(\theta)}\right|^2 \cos^2\left[\alpha_s^T(\theta_1) - \alpha_c^T(\theta) + \xi' - \zeta'\right] +$$

$$+ 4A\left|\frac{S_s^T(\theta)}{S_c^T(\theta)}\right| \left|\frac{S_s^T(\theta_1)}{S_c^T(\theta)}\right| \sin(kH\cos\theta) \cos\left[\alpha_s^T(\theta) - \alpha_c^T(\theta) - \zeta'\right] \times$$

$$\times \cos\left[\alpha_s^T(\theta_1) - \alpha_c^T(\theta_1) + \xi' - \zeta'\right] \quad , \tag{63}$$

$$\tan\alpha' = \frac{2A\left|\frac{S_s^T(\theta_1)}{S_c^T(\theta)}\right| \sin(kH\cos\theta) \cos\left[\alpha_s^T(\theta_1) - \alpha_c^T(\theta) + \xi' - \zeta'\right] \sin(\phi - \phi_1)}{\left|\frac{S_s^T(\theta)}{S_c^T(\theta)}\right| \cos\left[\alpha_s^T(\theta) - \alpha_c^T(\theta) - \zeta'\right] + 2A\left|\frac{S_s^T(\theta_1)}{S_c^T(\theta)}\right| \sin(kH\cos\theta) \left[\alpha_s^T(\theta_1) - \alpha_c^T(\theta) + \xi' - \zeta'\right] \cos(\phi - \phi_1)} \quad . \tag{64}$$

The bearing indication in the VOR receiver is

$$B = \phi - \alpha' = \phi + \Delta\phi \quad . \tag{65}$$

The bearing error $\Delta\phi$ in Eq. (65) is then given by:

$$\Delta\phi = -\tan^{-1}\left[\frac{2A\left|\frac{S_s^T(\theta_1)}{S_c^T(\theta)}\right| \sin(kH\cos\theta)\cos\left[\alpha_s^T(\theta_1) - \alpha_c^T(\theta) + \xi' - \zeta'\right]\sin(\phi-\phi_1)}{\left|\frac{S_s^T(\theta)}{S_c^T(\theta)}\right| \cos\left[\alpha_s^T(\theta) - \alpha_c^T(\theta) - \zeta'\right] + 2A\left|\frac{S_s^T(\theta_1)}{S_c^T(\theta)}\right| \sin(kH\cos\theta)\cos\left[\alpha_s^T(\theta_1) - \alpha_c^T(\theta) + \xi' - \zeta'\right]\cos(\phi-\phi_1)}\right] . \tag{66}$$

where,

$$\xi' = kd_1\left[1 - \sin\theta\sin\theta_1\cos(\phi-\phi_1)\right] + \delta - \pi/2 \tag{67}$$

$$\zeta' = \tan^{-1}\frac{2A\left|\frac{S_c^T(\theta_1)}{S_c^T(\theta_1)}\right| \sin(kH\cos\theta)\sin\left\{\xi' + \alpha_c^T(\theta_1) - \alpha_c^T(\theta)\right\}}{1 + 2A\left|\frac{S_c^T(\theta_1)}{S_c^T(\theta)}\right| \sin(kH\cos\theta)\cos\left\{\xi' + \alpha_c^T(\theta_1) - \alpha_c^T(\theta)\right\}} \tag{68}$$

3.3 Course Scalloping Amplitude

Proceedings in a manner discussed in Section 2.2, we obtain the following expressions for the course scalloping amplitudes:

$$S_1 = -\tan^{-1} \frac{2A \left| \frac{S_s^T(\theta_1)}{S_c^T(\theta)} \right| \sin(kH\cos\theta)\sin(\phi-\phi_1)}{\left| \frac{S_s^T(\theta)}{S_c^T(\theta)} \right| \cos\left[\alpha_s^T(\theta) - \alpha_c^T(\theta) - \zeta'_{01}\right] + 2A \left| \frac{S_s^T(\theta_1)}{S_c^T(\theta)} \right| \sin(kH\cos\theta)\cos(\phi-\phi_1)} \quad (69)$$

$$\zeta'_{01} = -\sin^{-1}\left[2A \left| \frac{S_c^T(\theta_1)}{S_c^T(\theta)} \right| \sin(kH\cos\theta)\sin\left(\alpha_s^T(\theta_1) - \alpha_c^T(\theta_1)\right)\right] \quad (70)$$

and,

$$S_2 = \tan^{-1} \frac{2A \left| \frac{S_c^T(\theta_1)}{S_c^T(\theta)} \right| \sin(kH\cos\theta)\sin(\phi-\phi_1)}{\left| \frac{S_s^T(\theta)}{S_c^T(\theta)} \right| \cos\left[\alpha_s^T(\theta) - \alpha_c^T(\theta) - \zeta'_{02}\right] - 2A \left| \frac{S_s^T(\theta_1)}{S_c^T(\theta)} \right| \sin(kH\cos\theta)\cos(\phi-\phi_1)} , \quad (71)$$

$$\zeta'_{02} = \sin^{-1}\left[2A \left| \frac{S_c^T(\theta_1)}{S_c^T(\theta)} \right| \sin(kH\cos\theta)\sin\left\{\alpha_s^T(\theta_1) - \alpha_c^T(\theta_1)\right\}\right] . \quad (72)$$

If $\alpha_s^T(\theta) = \alpha_c^T(\theta)$, i.e., if the phase of the carrier mode complex elevation

plane pattern is equal to the phase of the side-band complex elevation plane pattern, then $\zeta'_{01} = \zeta'_{02} = 0$ and Eq. (69) and (71) reduce to the following:

$$S_1 = -\tan^{-1}\left[\frac{2A\left|S_s^T(\theta_1)\right| \sin(kH\cos\theta)\sin(\phi-\phi_1)}{\left|S_s^T(\theta)\right| + 2A\left|S_s^T(\theta_1)\right| \sin(kH\cos\theta)\cos(\phi-\phi_1)}\right], \tag{73}$$

$$S_2 = \tan^{-1}\left[\frac{2A\left|S_s^T(\theta_1)\right| \sin(kH\cos\theta)\sin(\phi-\phi_1)}{\left|S_s^T(\theta)\right| - 2A\left|S_s^T(\theta_1)\right| \sin(kH\cos\theta)\cos(\phi-\phi_1)}\right]. \tag{74}$$

Equations (73) and (74) indicate that for orbital flights

S_1 evaluated at $\pi + (\phi-\phi_1) = S_2$ evaluated at $(\phi-\phi_1)$,

S_2 evaluated at $\pi + (\phi-\phi_1) = S_1$ evaluated at $(\phi-\phi_1)$.

The above relations imply that it is sufficient to calculate S_1 and S_2 in the range $0 \leq (\phi-\phi_1) \leq \pi$ in order to study the course scalloping amplitude variations during an orbital flight.

It is also interesting to observe from Eqs. (73) and (74) that the course scalloping amplitude reduces to zero whenever the following relation holds:

$$H\cos\theta = {}^{n\lambda}/_{2}, \quad n = 1, 2, 3, \ldots \tag{75}$$

3.4 Discussion

The general expressions for the course scalloping amplitudes in the standard VOR receiver bearing indications are given by Eqs. (69) and (71). The theory clearly indicates that the course scalloping amplitudes depend on the following parameters: (a) the amplitude $A(\theta_1, \phi_1, d_1; \theta, \phi)$ of the scattering coefficient of the multipath source located at (d_1, θ_1, ϕ_1), (b) the amplitude and phase of the carrier and side-band mode elevation plane complex patterns of the standard VOR antenna, (c) the location of the multipath source with respect to the VOR station.

After studying the scalloping amplitude expressions, the following observations can be made with regard to the general behavior of the course scalloping amplitudes in the VOR bearing indications observed by an aircraft in orbital flight around the VOR station:

(i) The scalloping amplitude is zero in directions $\phi = \phi_1$ and $\phi = \pi + \phi_1$. If the multipath source scatters energy isotropically (i.e., A = constant) then the amplitude of scattering assumes maximum value in directions $\phi = \pi/2 + \phi_1$ and $\phi = 3\pi/2 + \phi_1$, only if $A \ll 1$.

(ii) The two envelopes of the bearing error (S_1, S_2) are opposite in sign but in general are not equal in amplitude.

(iii) In the case of a non-isotropic scattering behavior of the multipath source, the directions of the scalloping amplitude maxima will be determined mainly by the parameter A.

(iv) The side-band mode pattern $\left|S_s^T(\theta)\right|$ is quite critical in determining the scalloping amplitudes. The scalloping amplitude increases in the directions of minima in the pattern $\left|S_s^T(\theta)\right|$. $\left|S_c^T(\theta)\right|$ does not seem to have strong influence on $|S_1|$ and $|S_2|$. However, the relative phase difference between the side-band and carrier mode fields $(\alpha_s^T(\theta) - \alpha_c^T(\theta)$ influences considerably the amount of scalloping amplitudes.

(v) $|S_1|$ and $|S_2|$ decreases with increase of d_1, where (d_1, θ_1, ϕ_1) are the coordinates of the multipath source.

(vi) $|S_1|$ and $|S_2|$ increases with increase of height H of the multipath source when the aircraft is flying at low elevation angle from the horizon.

All of the above observations are in qualitative agreement with the observed course scalloping amplitude data discussed in [2] and [4].

IV

RF PHASE RELATIONSHIP BETWEEN CARRIER AND SIDE-BAND SIGNALS

It was mentioned earlier that the r.f. phase relationship between the received side-band and carrier signals plays an important role in the detection efficiency of the VOR receiver at the aircraft. From the scalloping expressions developed in the previous sections it is also found that the same phase relationship has considerable effects on the observed course scalloping amplitudes. For an antenna located in free space this phase difference may be represented by $\alpha_s(\theta) - \alpha_c(\theta)$ where $\alpha_s(\theta)$ and $\alpha_c(\theta)$ are the phase angles of the side-band and carrier complex patterns respectively, as defined by Eqs. (3) and (2). For an antenna located above infinite planar ground the phase difference is represented by $\alpha_s^T(\theta) - \alpha_c^T(\theta)$ where $\alpha_s^T(\theta)$ and $\alpha_c^T(\theta)$ are as defined by Eq. (60).

The results discussed in the previous sections indicate that in general if $\alpha_c(\theta) = \alpha_s(\theta)$ $\left[\text{or } \alpha_c^T(\theta) = \alpha_s^T(\theta)\right]$ for all θ, then the detection efficiency is maximum and also the observed course scalloping would be minimum. It is therefore important to study the variation of the r.f. phase difference between the two signals as a function of θ for a given antenna. Complete expressions for the carrier and side-band mode complex patterns of various standard VOR antennas have been given in [6]-[8]. Here we discuss only the variations of the phases of the complex patterns as functions of θ.

Figure 4 shows the variations of $\alpha_c(\theta)$, $\alpha_s(\theta)$ and $\alpha_s(\theta) - \alpha_c(\theta)$ as functions of θ for a standard VOR antenna located in free space. The corresponding results for a standard VOR antenna located 15' above an infinite planar ground are shown in Fig. 5. Figures 6 and 7 show the corresponding results for a large gradient parasitic loop counterpoise antenna under similar conditions. For the standard VOR antenna it is found that the phase difference is almost constant for all θ in both cases. For the parasitic antenna case the phase difference is found to be reasonably constant in the range $55^\circ \leq \theta \leq 95^\circ$ for the free space case; the phase difference fluctuates with an average value near 100° for $50^\circ \leq \theta \leq 85^\circ$ for the

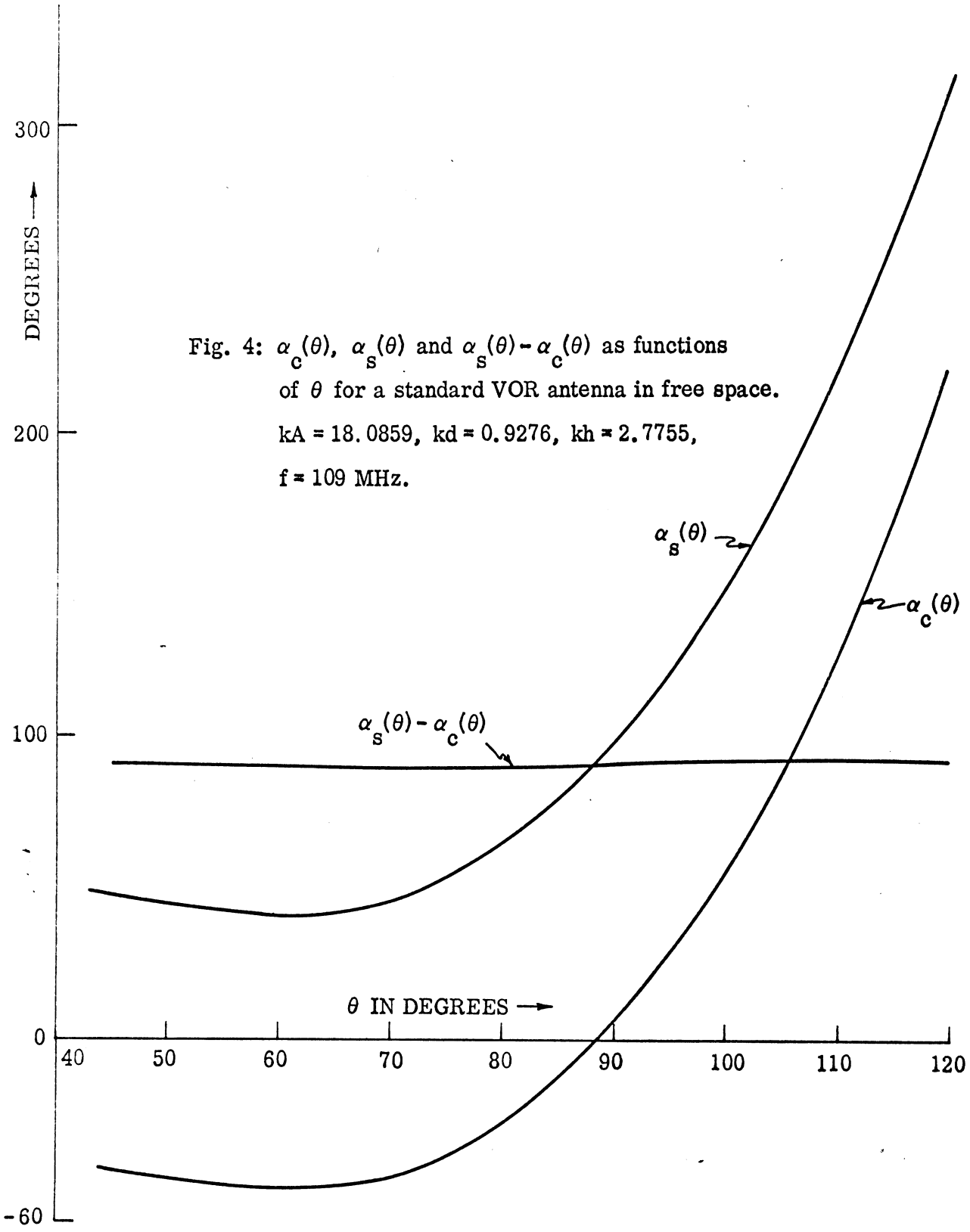

Fig. 4: $\alpha_c(\theta)$, $\alpha_s(\theta)$ and $\alpha_s(\theta) - \alpha_c(\theta)$ as functions of θ for a standard VOR antenna in free space. kA = 18.0859, kd = 0.9276, kh = 2.7755, f = 109 MHz.

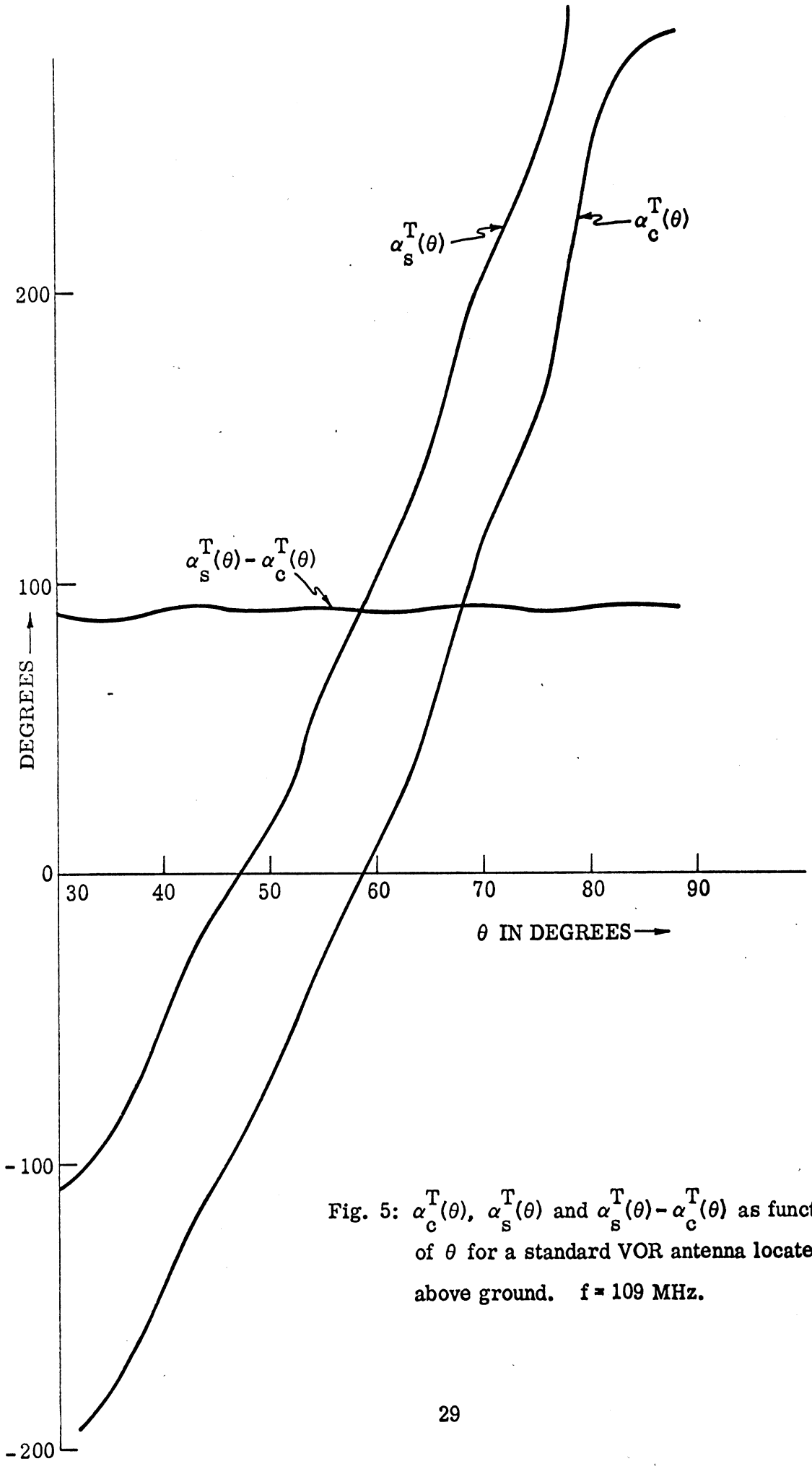

Fig. 5: $\alpha_c^T(\theta)$, $\alpha_s^T(\theta)$ and $\alpha_s^T(\theta) - \alpha_c^T(\theta)$ as functions of θ for a standard VOR antenna located 15' above ground. f = 109 MHz.

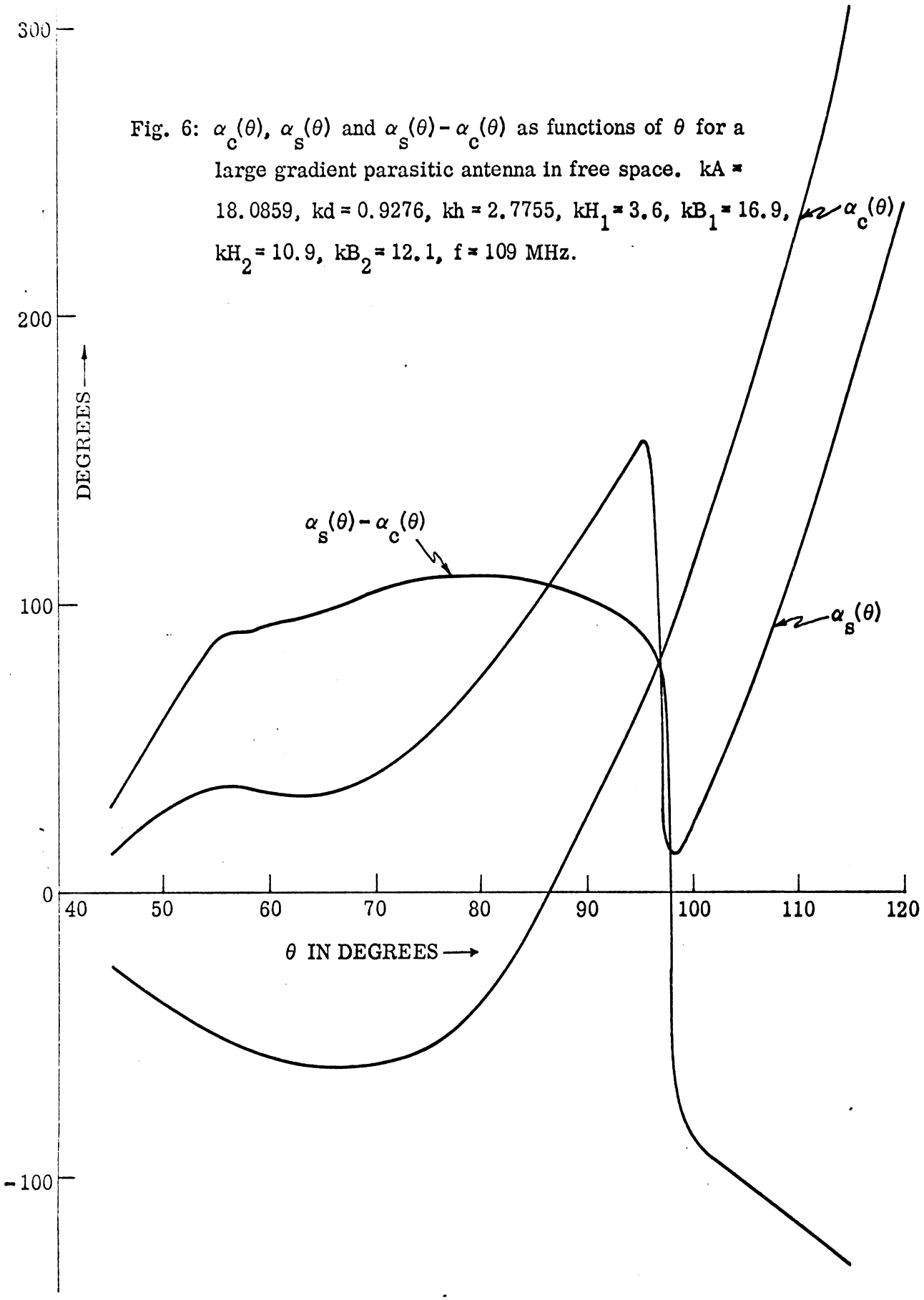

Fig. 6: $\alpha_c(\theta)$, $\alpha_s(\theta)$ and $\alpha_s(\theta) - \alpha_c(\theta)$ as functions of θ for a large gradient parasitic antenna in free space. kA = 18.0859, kd = 0.9276, kh = 2.7755, $kH_1 = 3.6$, $kB_1 = 16.9$, $kH_2 = 10.9$, $kB_2 = 12.1$, f = 109 MHz.

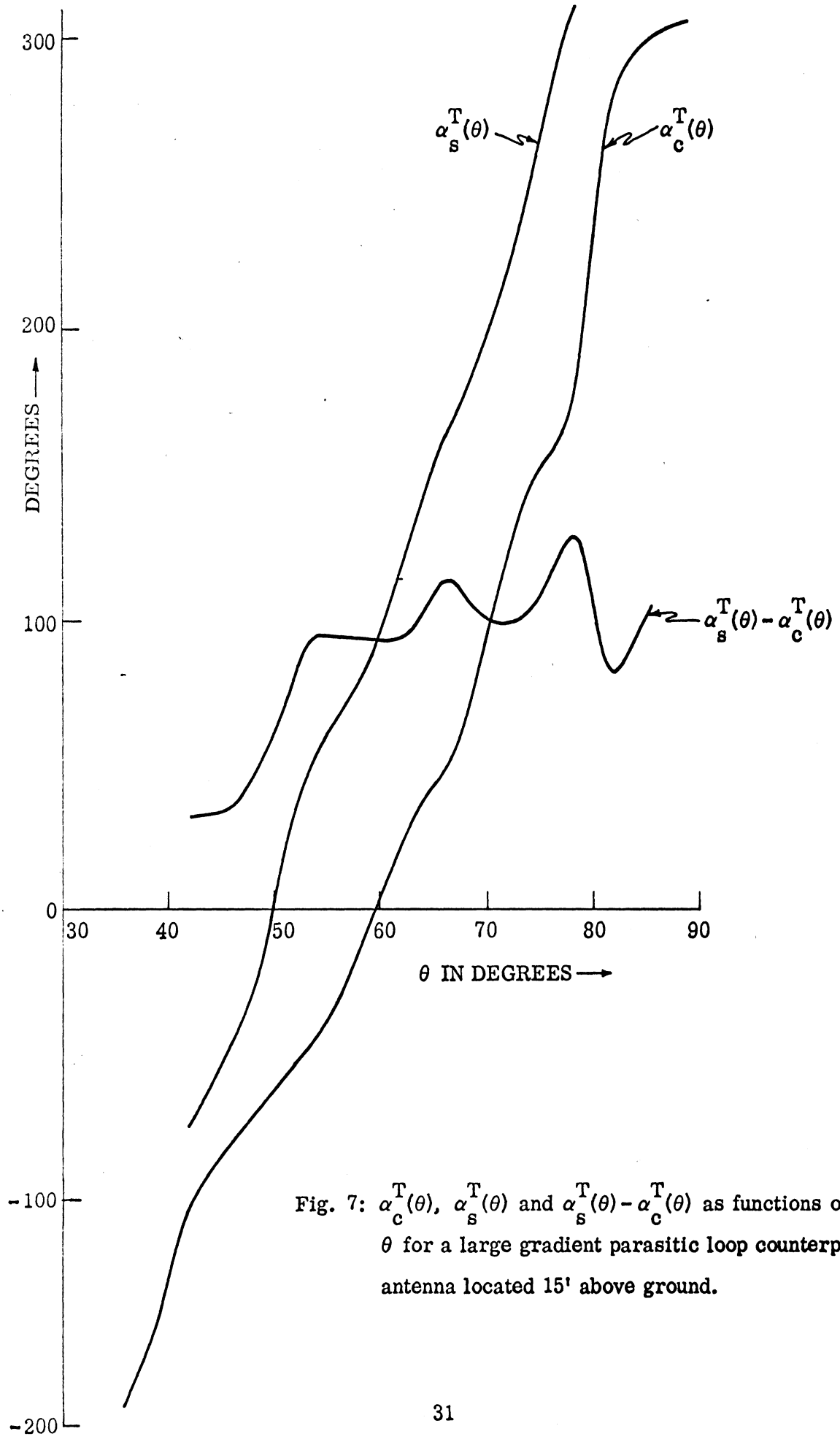

Fig. 7: $\alpha_c^T(\theta)$, $\alpha_s^T(\theta)$ and $\alpha_s^T(\theta) - \alpha_c^T(\theta)$ as functions of θ for a large gradient parasitic loop counterpoise antenna located 15' above ground.

same antenna located above ground.

On the basis of the results given here it can be concluded that it is sufficient to adjust the r.f. phase between the carrier and side-band signals radiated by a standard VOR antenna at a certain convenient angle (say, at the monitor). With a parasitic loop counterpoise antenna it appears that the r.f. phase difference between the two signals cannot be maintained at zero for all angles by such simple adjustment.

V

NUMERICAL RESULTS FOR COURSE SCALLOPING AMPLITUDES

In this section we discuss the numerical results obtained for the observed course scalloping amplitudes in a standard VOR indications for some selected cases. The results have been obtained numerically by using the expressions developed in sections 2 and 3.

In the free space case the observed course scalloping amplitudes are given by Eqs. (35) and (36). For convenience we rewrite them in the following form:

$$S_{\substack{1\\2}} = \mp \tan^{-1}\left[\frac{A \sin(\phi-\phi_1)}{1 \pm A\cos(\phi-\phi_1)}\right], \tag{75}$$

where the upper and the lower sign on the right hand side corresponds respectively to the subscripts 1 and 2 on the left hand side. The various approximations involved in obtaining Eq. (75) have been discussed earlier. In reference [2], further approximation $A \ll 1$ is made in order to obtain the following from Eq. (71)

$$S_{\substack{1\\2}}^{\text{Approx}} = \mp \tan^{-1} A\sin(\phi-\phi_1) \quad . \tag{76}$$

Figure 8 shows $|S_1|$ and $|S_1^{\text{Approx}}|$ vs. $(\phi-\phi_1)$ in the range $0 \leq \phi-\phi_1 \leq 180^\circ$ for two values of A. It is evident from Fig. 8 that for $A \leq 0.1$ the use of the approximate expressions give by Eq. (76) is quite justified. For $A > 0.1$ the use of Eq. (76) will produce erroneous results. For example, Fig. 8 indicates that with $A = 0.2$ the maximum scalloping amplitude does not occur at $\phi-\phi_1 = \pi/2$. In fact for large values of A the symmetry of the scalloping amplitude curves around $\phi-\phi_1 = \pi/2$ are lost and the maxima appear at angles larger than $\pi/2$.

In the following sections we discuss the numerical results obtained for the observed course scalloping amplitudes for a standard VOR system located above an infinite planar ground. The scalloping amplitudes have been obtained numerically

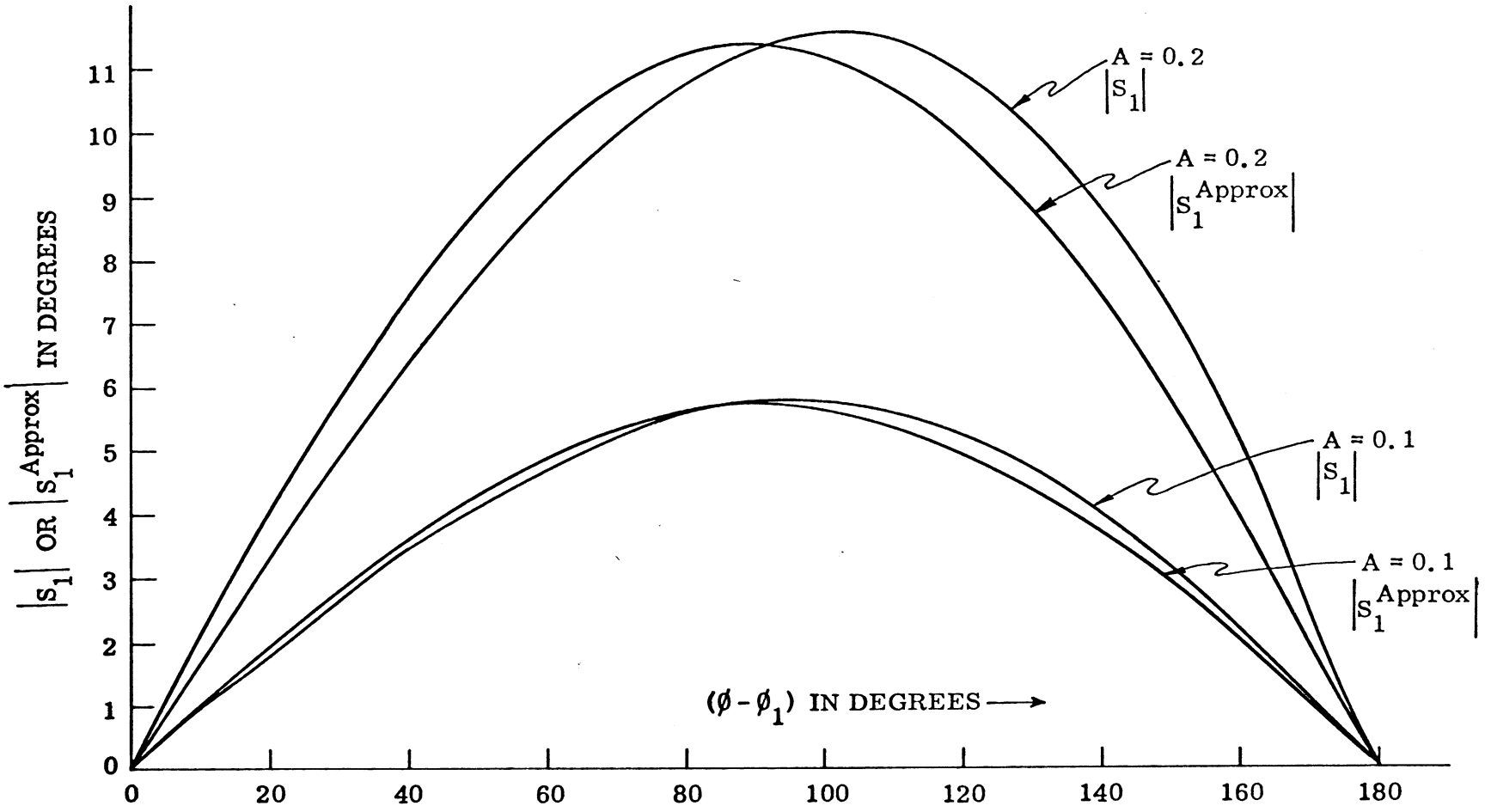

Fig. 8: Free space scalloping amplitudes $|S_1|$ and $|S_1^{Approx}|$ as functions of $(\phi - \phi_1)$ with A as the parameter.

from Eqs. (73) and (74) which we write below in the following form:

$$S_{\substack{1\\2}} = \mp \tan^{-1}\left[\frac{|2A|\,|S_s^T(\theta_1)|\,\sin(kH\cos\theta)\sin(\phi-\phi_1)}{|S_s^T(\theta)| \pm 2A|S_s^T(\theta_1)|\,\sin(kH\cos\theta)\cos(\phi-\phi_1)}\right] \tag{77}$$

Notice that Eq. (77) indicates explicitly the dependence of the scalloping amplitude on the side-band mode pattern of the antenna and the height of the scatterer above ground. In obtaining Eq. (77) it has been assumed that the r.f. phase of the carrier mode complex pattern is equal to that of the side-band mode complex pattern. For the present discussion we consider the cases when the standard VOR system uses a standard VOR antenna and a large gradient ($23\text{dB}/6^\circ$ gradient) parasitic loop counterpoise antenna. In both cases the antenna is assumed to be located 15' above the ground and the operating frequency is 109 MHz.

In our first quarterly report [9] it has been shown that the side-band mode pattern $S_s^T(\theta)$ for a standard VOR antenna located 15' above ground contains a local minimum at $\theta = \theta_{min} \sim 76^\circ$ and a local maximum at $\theta = \theta_{max} \sim 83^\circ$. For the large gradient antenna at the same height $S_s^T(\theta)$ does not have any appreciable maximum of minimum in this region. We compare the observed scalloping amplitudes with both antennas for orbital flights at these two angles. It is assumed that the scattering source is isotropic and that $A = 0.1$.

Figures 9(a) and 9(b) show $|S_1|$ and $|S_2|$ as functions of $(\phi - \phi_1)$ for the standard VOR antenna located 15' above ground for the scatterer located at different heights above ground. These results apply to an orbital flight around the station at $\theta = \theta_{min} \sim 76^\circ$. Corresponding results for the same antenna for an orbital flight at $\theta = \theta_{max} \sim 83^\circ$ are shown in Figs. 10(a) and 10(b). In general it is found that the scalloping amplitudes are less for $\theta = \theta_{max}$.

Corresponding results for the large gradient parasitic loop counterpoise antenna are shown in Figs 11(a) and 11(b) for orbital flights at $\theta = \theta_{min}$. In comparing Figs. 11 and 9 it is found that the large gradient system produces smaller

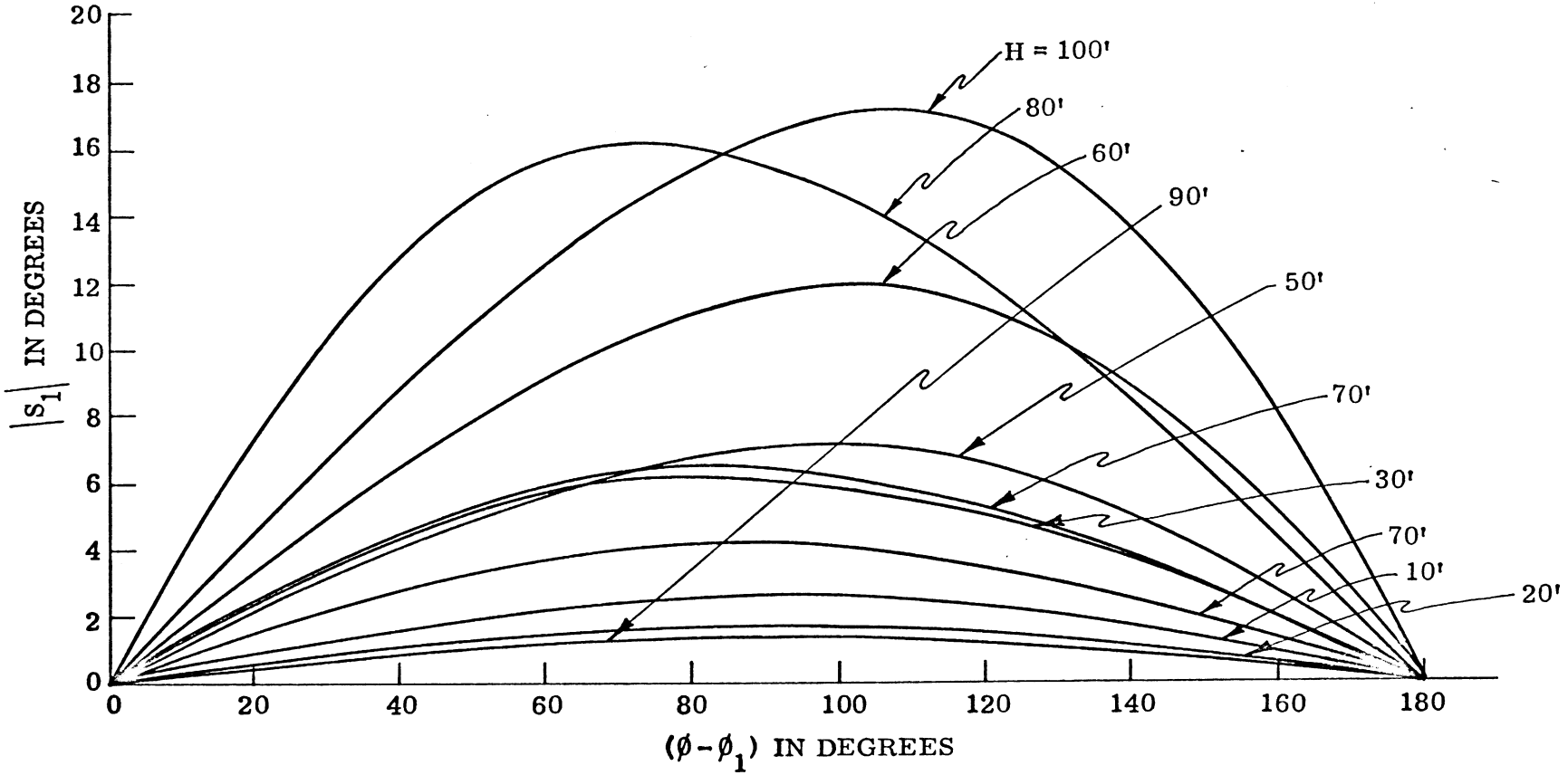

Fig. 9(a): Course scalloping amplitude $|S_1|$ as a function of $(\phi - \phi_1)$ for a standard VOR antenna located 15' above ground and for different heights of the scatterer. Orbital flight at $\theta = \theta_{min} \sim 76^{\circ}$.

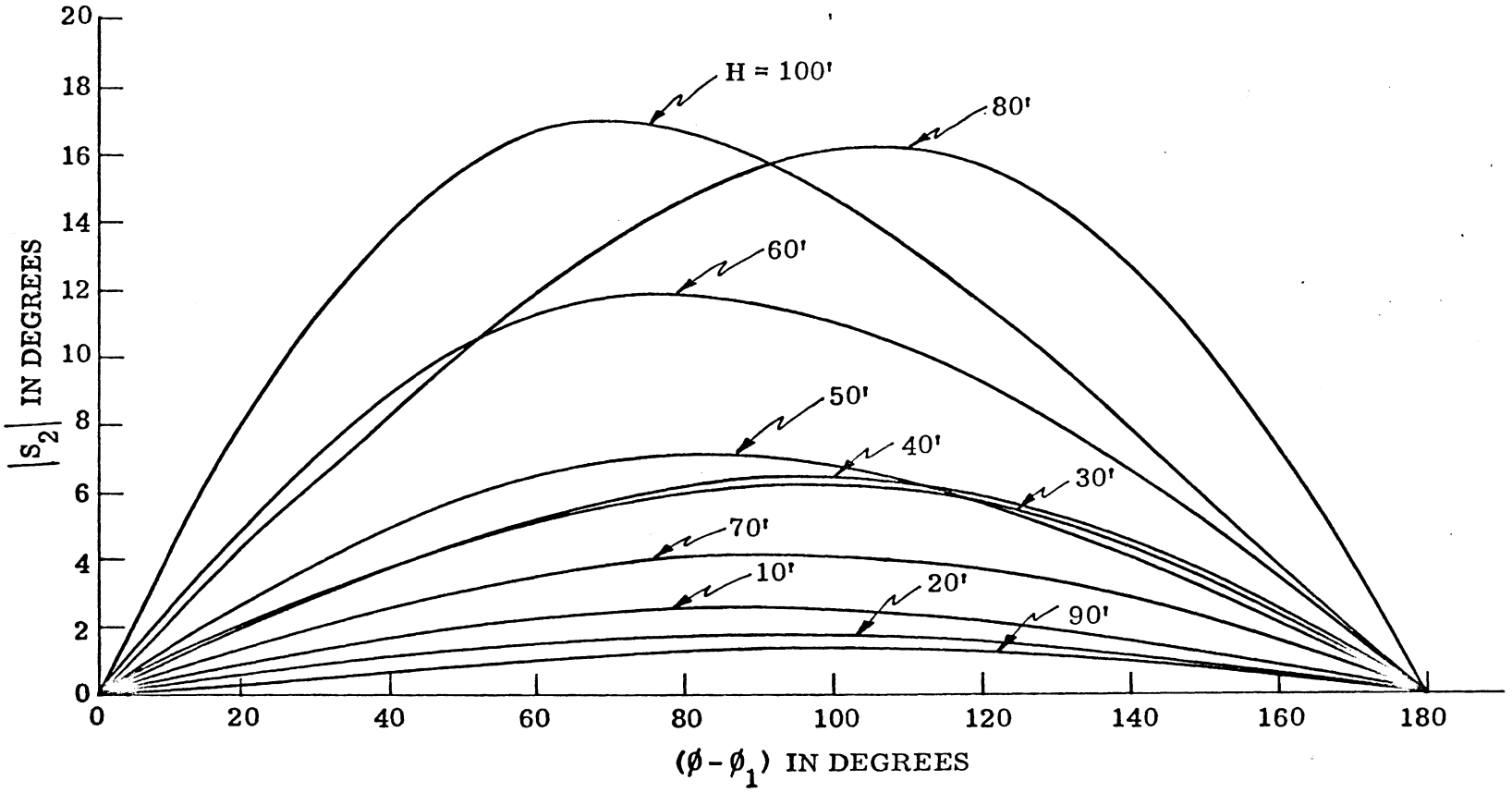

Fig. 9(b): Course scalloping amplitude $|S_2|$ as a function of $(\phi - \phi_1)$ for a standard VOR antenna located 15' above ground and for different heights of the scatterer. Orbital flight at $\theta = \theta_{min} \sim 76^{\circ}$.

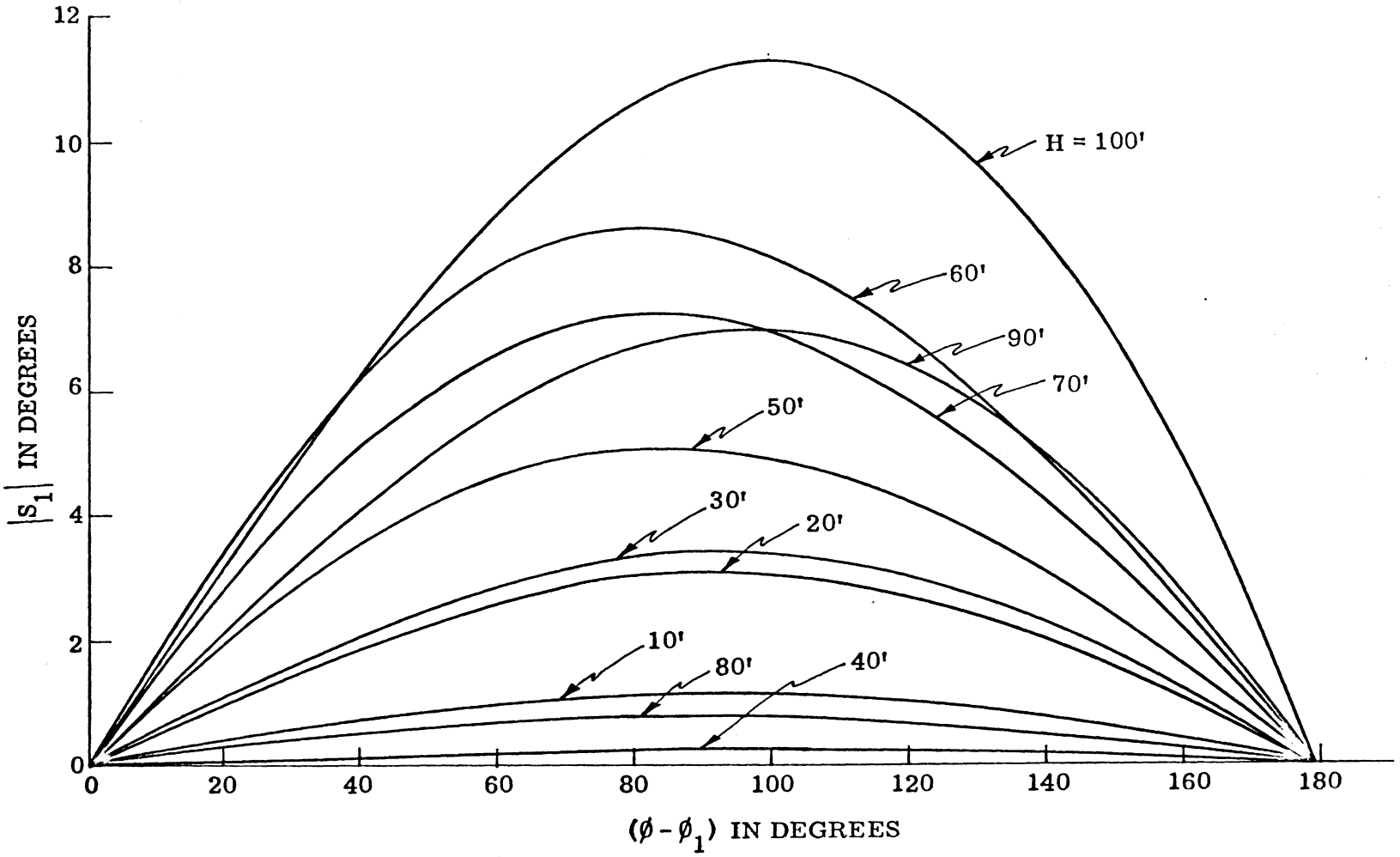

Fig. 10(a): Course scalloping amplitude $|S_1|$ as a function of $(\phi - \phi_1)$ for a standard VOR antenna located 15' above ground and for different heights of the scatterer. Orbital flight at $\theta = \theta_{max} \sim 83^{\circ}$.

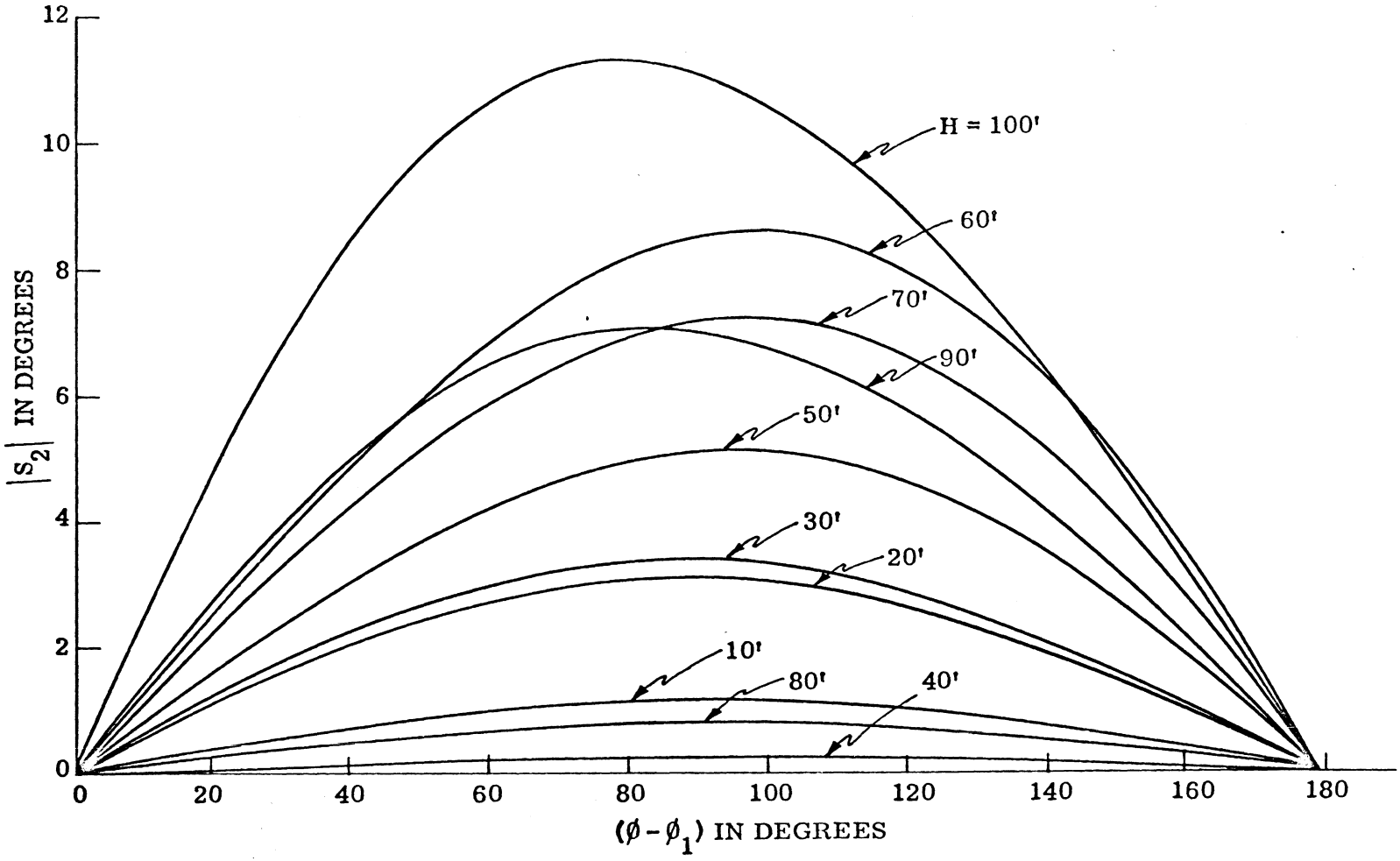

Fig. 10(b): Course scalloping amplitude $|S_2|$ as a function of $(\phi - \phi_1)$ for a standard VOR antenna located 15' above ground and for different heights of the scatterer. Orbital flight at $\theta = \theta_{max} \sim 83^{\circ}$.

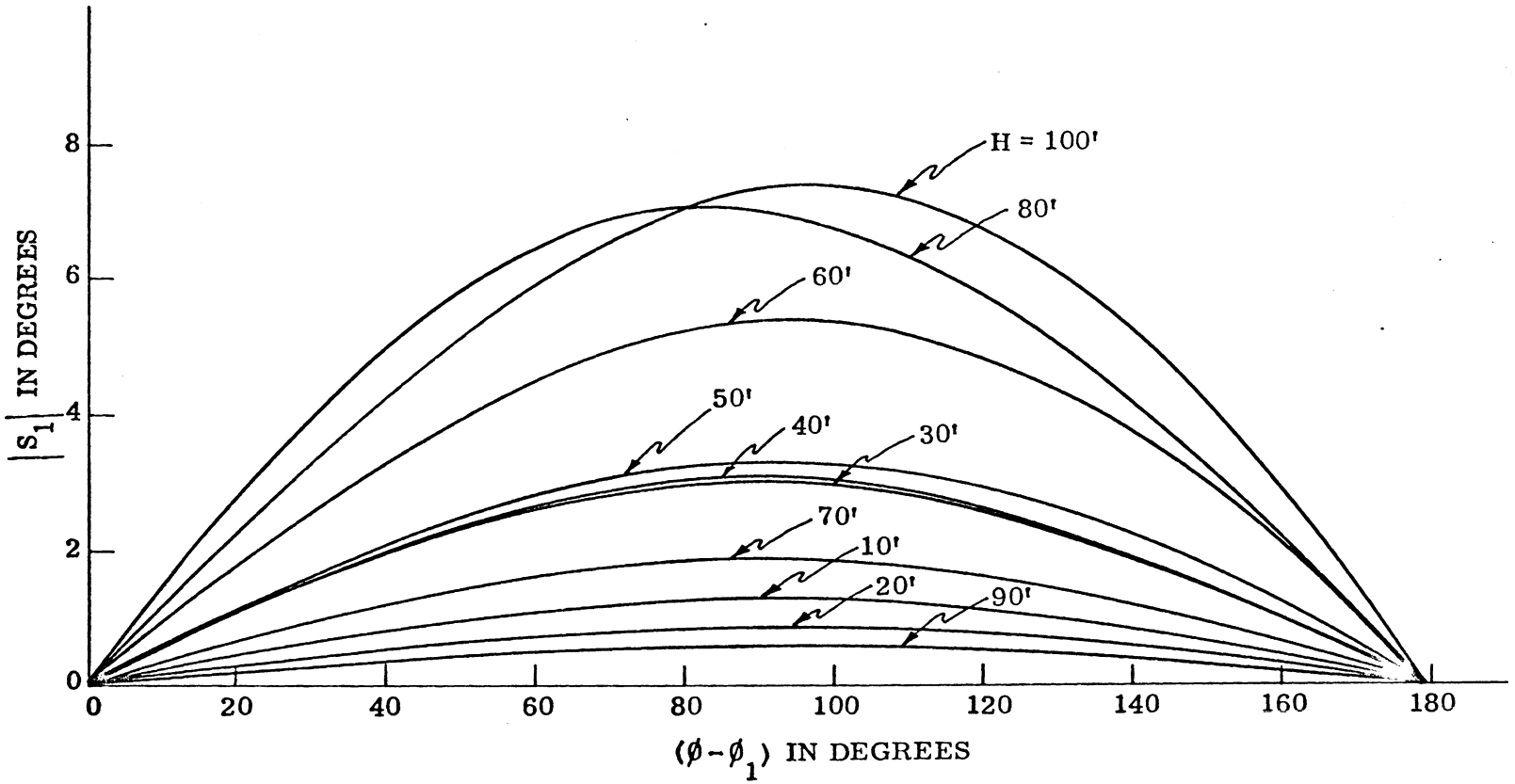

Fig. 11(a): Course scalloping amplitude $|S_1|$ as a function of $(\phi - \phi_1)$ for a large gradient parasitic loop counterpoise antenna located 15' above ground and for different heights of the scatterer. Orbital flight at $\theta = 76^{\circ}$.

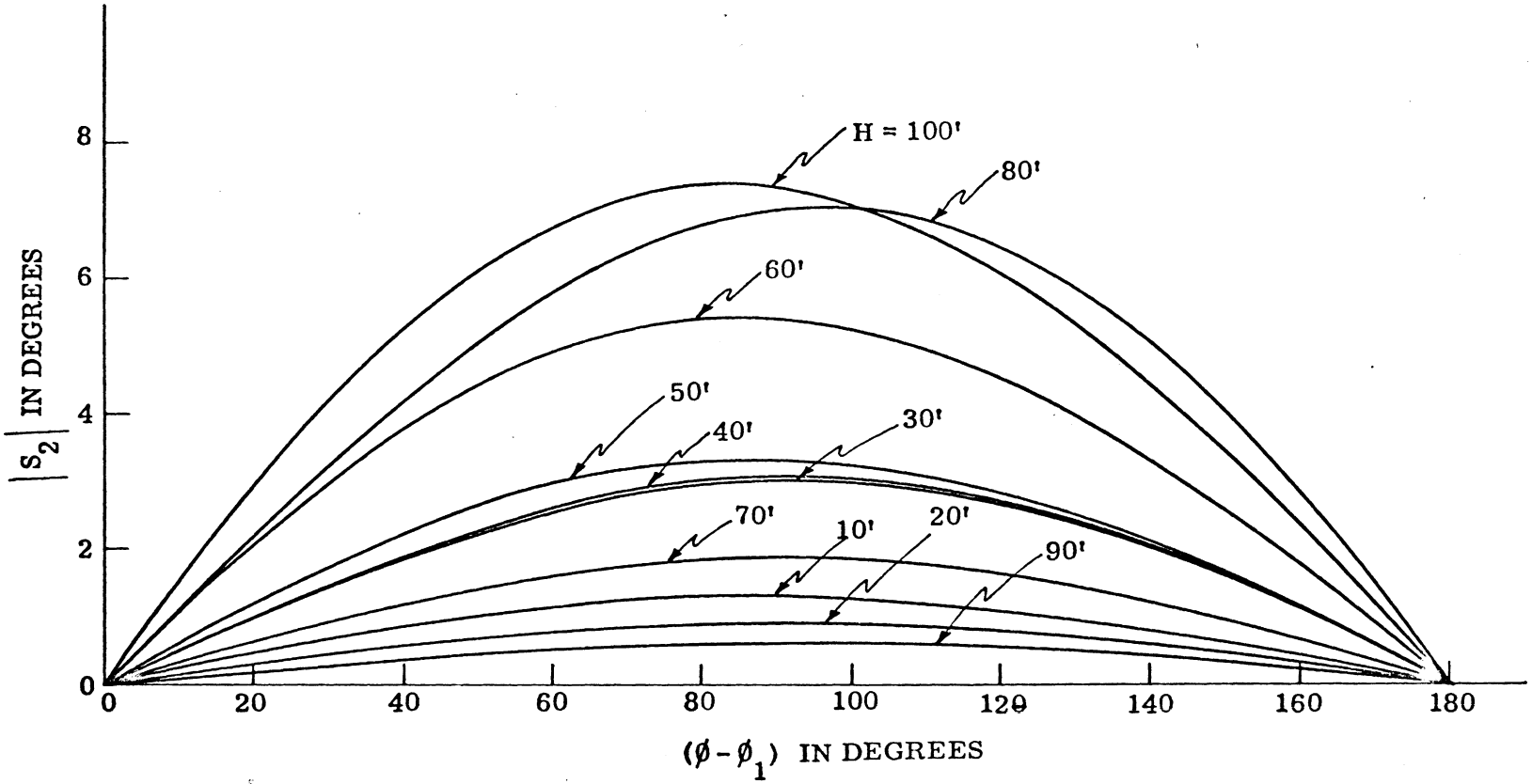

Fig. 11(b): Course scalloping amplitude $|S_2|$ as a function of $(\phi - \phi_1)$ for a large gradient parasitic loop counterpoise antenna located 15' above ground and for different heights of the scatterer. Orbital flight at $\theta = 76^{\circ}$.

course scalloping amplitudes. This is attributed to the large gradient possessed by the vertical plane side-band mode pattern of the parasitic antenna.

Figure 12 shows $|S_2|$ vs. $(\phi - \phi_1)$ for standard VOR and large gradient antennas located 15' above ground and for orbital flights at $\theta = \theta_{max} \sim 83^{o}$. In both cases the scatterer is located 100' above ground. Observe that in this case the difference between the two scalloping amplitudes may be assumed to be negligible except near the maxima where it is about 0.5^{o}.

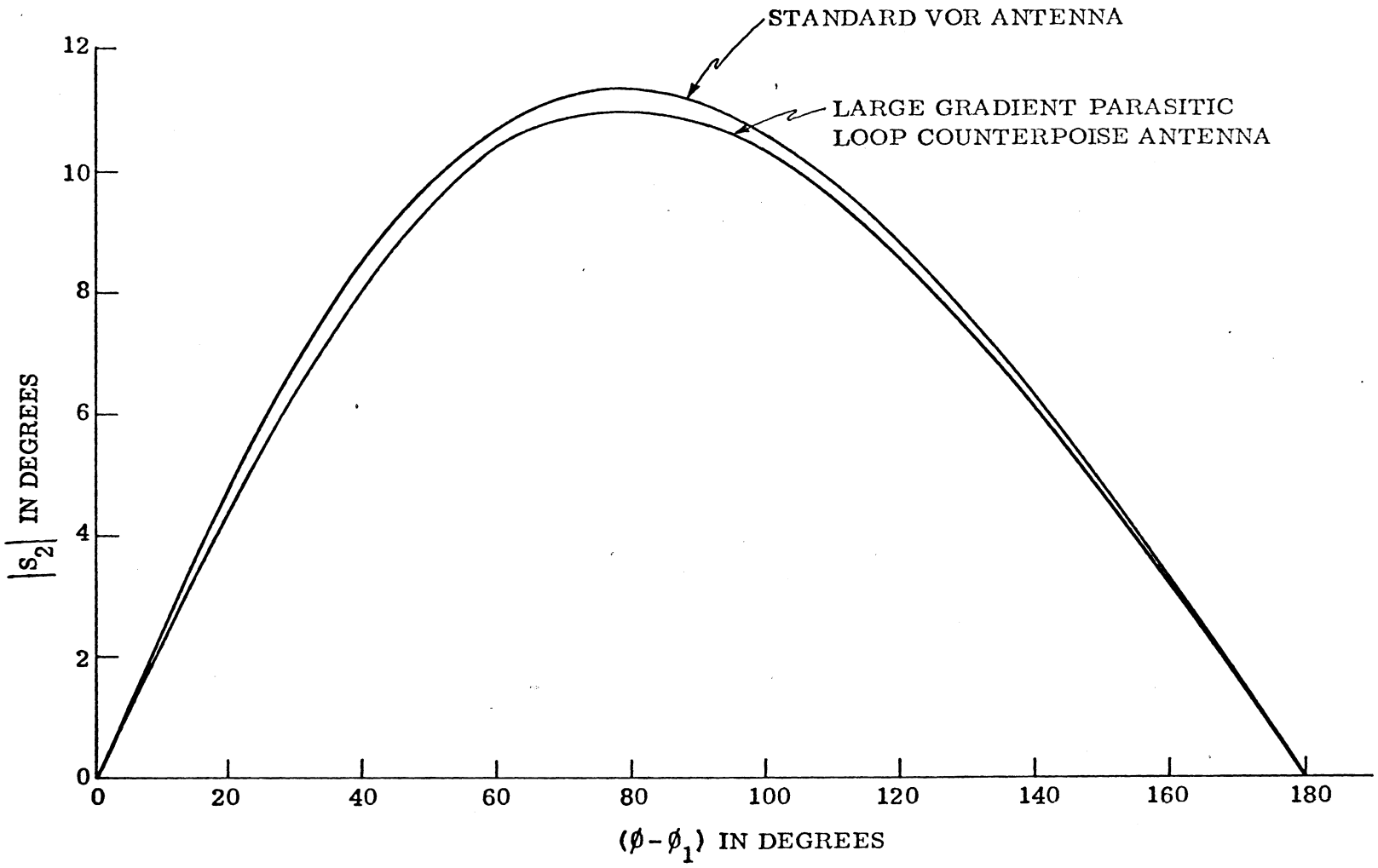

Fig. 12: Course scalloping amplitudes $|S_2|$ as functions of $(\phi - \phi_1)$ for a standard VOR and large gradient parasitic loop counterpoise antennas located 15' above ground for a scatterer located 100' above ground. Orbital flight at $\theta = 83^{\circ}$.

VI

CONCLUSIONS

A rigorous theory has been developed for the course scalloping amplitudes in the bearing indications of a standard VOR receiver located at a flying aircraft. The receiver characteristics have been assumed to be ideal. The general behavior of the available observed scalloping amplitude amplitude results appears to be in agreement with the theory. Numerical results have been obtained for the idealized case of an isotropic scatterer located at various heights above ground. The results indicate that in general the use of a large gradient antenna reduces the observed scalloping amplitudes.

During the coming period numerical results will be obtained for various heights of the VOR antennas and the scattering object above ground. Thoughts also will be given to the case of more realistic scatterers, i. e., non-isotropic multipath sources and also to the influence of the detailed scattering properties of the multipath source on the scalloping amplitudes.

VII

REFERENCES

[1] Anderson, S. R., VHF OmniRange Accuracy Improvements, IEEE Trans. on Aerospace and Navigational Electronics, Vol. AME-12, No. 1, pp. 26-35, 1965.

[2] Handbook, VOR/VORTAC Siting Criteria, No. 6700.11, Department of Transportation, Federal Aviation Administration, Washington, D. C., August 7, 1968.

[3] Anderson, S. R. and H. F. Keary, VHF Omnirange Wave Reflections from Wires, Technical Development Report No. 126, Civil Aeronautics Administration Technical Development and Evaluation Center, Indianapolis, Indiana, 1952.

[4] Electro Technical Analysis Corporation, Analysis of Vector Analogue Computer, Final Report No. RD-67-37, P. O. Box 5741, Tucson, Arizona 85703.

[5] Sengupta, D. L., Theory of Course Scalloping Amplitude in Standard VOR Bearing Indications--Part I--Analysis., Radiation Laboratory Memorandum 011218-501-M, September 1972.

[6] Sengupta, D. L. and V. H. Weston, Investigation of the Parasitic Loop Counterpoise Antenna, IEEE Trans., AP-17, No. 2, pp. 180-191, 1969.

[7] Sengupta, D. L., Theory of VOR Antenna Radiation Patterns, IEE (London) Electronics Letters, Vol. 7, No. 5, pp. 418-420, 1971.

[8] Sengupta, D. L., Theory of Double Parasitic Loop Counterpoise Antenna Radiation Patterns, IEEE Trans., AP-21, No. 1, pp. 94-97, 1973.

[9] Sengupta, D. L. and P. Chan, Application of the Large Gradient VOR Antenna, Interim Engineering Report I, 011218-1-T, University of Michigan Radiation Laboratory, September 1972.